

Extended and revised analysis of singly ionized tin: Sn II

K Haris¹, A Kramida² and A Tauheed¹

¹Department of Physics, Aligarh Muslim University, Aligarh 202002, India

²National Institute of Standards and Technology, Gaithersburg, MD 20899, USA

E-mail: alexander.kramida@nist.gov

December 1, 2013

Abstract. The electronic structure of singly ionized tin (Sn II) is partly a one-electron and partly a three-electron system with ground configuration $5s^25p$. The excited configurations are of the type $5s^2n\ell$ in the one-electron part, and $5s5p^2$, $5p^3$ and $5s5pn\ell$ ($n\ell = 6s, 5d$) in the three-electron system with quartet and doublet levels. The spectrum analyzed in this work was recorded on a 3 m normal incidence vacuum spectrograph of the Antigonish laboratory (Canada) in the wavelength region 300 Å to 2080 Å using a triggered spark source. The existing interpretation of the one-electron level system was confirmed in this paper, while the $^2S_{1/2}$ level of the $5s5p^2$ configuration has been revised. The analysis has been extended to include new configurations $5p^3$, $5s5p5d$ and $5s5p6s$ with the aid of superposition-of-configurations Hartree–Fock calculations with relativistic corrections. The ionization potential obtained from the ng series was found to be $118023.7(5) \text{ cm}^{-1}$ ($14.63307(6) \text{ eV}$). We give a complete set of critically evaluated data on energy levels, observed wavelengths and transition probabilities of Sn II in the range 888 Å to 10740 Å involving excitation of the $n = 5$ electrons.

PACS numbers: 32.10.Fn, 32.10.Hq, 32.30.Jc, 32.70.Cs, 32.70.Fw

(Some figures may appear in colour only in the online journal)

1. Introduction

Accurate data on the spectrum of singly ionized tin are needed in different fields of scientific research and industry. Such data are useful for astrophysical observations, development of various light sources, and for plasma diagnostics in fusion power plants. The astrophysical importance of tin has increased since gas-phase tin was first detected by Hobbs et al. [1] in the spectra acquired with the Goddard High Resolution Spectrograph on board the Hubble Space Telescope. They observed the absorption line of Sn II at 1400.45 Å from various interstellar sources. Later, the same line was observed in diffuse interstellar clouds by Sofia et al. [2]. They discovered that the gas-phase abundance of Sn in the interstellar medium (ISM) appears to be supersolar, which further substantiates the slow neutron capture (s-process) enrichment believed to be a major contributor to the nucleosynthesis of elements beyond the iron peak in the ISM. In erosion probing of vessel wall tiles of future fusion power plants, such as ITER, spectroscopic data on tin may play a major diagnostic role [3].

Singly ionized tin (Sn II) is the second member of the In I isoelectronic sequence with the ground configuration $4d^{10}5s^25p$ consisting of the ground level $^2P^{\circ}_{1/2}$ and first excited level $^2P^{\circ}_{3/2}$. The currently available spectroscopic information on Sn II compiled in Moore's Atomic Energy Levels (AEL) compilation [4] and listed in the Atomic Spectra Database (ASD) [5] of the National Institute of Standards and Technology (NIST) is based on an unpublished work of Shenstone. Prior to AEL, extensive work in this spectrum was carried out by McCormick and Sawyer [6], who revised the earlier findings of Green and Loring [7], Narayan and Rao [8], and Lang [9]. Shenstone in his work quoted in AEL re-investigated this spectrum in the wavelength range of 600 Å to 2500 Å and extended the analysis to include the $5s5p5d$ and $5s5p6s$ configurations. Shenstone revised some energy levels of Sn II and improved the accuracy of the earlier reported energy level values on the basis of his observations. Some spectral lines of Sn II were also reported by Brill [10] in his doctoral thesis and by Wu [11] in his master thesis. Apart from spectroscopy of valence-shell electrons, spectral studies of the 4d-core excitation of

Sn II in the extreme ultraviolet (EUV) region with the dual laser plasma (DLP) method were made by Lysaght et al. [12] and by Duffy et al. [13].

Despite those extensive studies, the currently available data are still inadequate, since there are considerable anomalies in energy level values and line assignments. Many of the energy levels given in AEL [4] are not supported by any published line lists. The lines determining these energy levels have to be re-discovered.

There are many theoretical studies on radiative lifetimes, transition rates, and oscillator strengths of Sn II. Among them, the most accurate and reliable work was done by Oliver and Hibbert [14]. Accurate lifetime measurements, and thereby f -value determinations, were made by Schectman et al. [15] who improved the earlier work of Andersen and Lindgård [16]. Data from the latter work were used by Sofia et al. [2] to derive the abundance of tin.

In the present work, our motivation is to provide a comprehensive spectroscopic analysis of singly ionized tin on the basis of tin spectra taken by us, the tin spectral line list given by Wu [11], the Sn II spectral classification by McCormick and Sawyer [6], and lines reported by Brill [10]. All previously reported energy levels of this spectrum are subjected to a critical investigation. One of our goals is to resolve the anomaly existing in the $5s5p^2\ ^2S_{1/2}$ and $^2P_{1/2}$ level values. Excitation from the $5s5p^2$ configuration to $5s5p(5d+6s)$ and $5p^3$ is studied extensively in this work. Although some of the levels of these highly-excited configurations were tentatively identified by Shenstone and listed in AEL [4], Shenstone's analysis was incomplete in many respects. Some of the level values were given with question marks, and some had uncertain J values and/or designations. A very recent study carried out by Alonso-Medina et al. [17] using laser-produced plasma of a Sn/Pb target reproduced some of the levels reported in AEL [4], but the majority of their suggested $5s5p5d$ level assignments and line classifications are made on the basis of a physically inadequate theoretical atomic model. We attempt to resolve all these ambiguities in the present analysis. Interestingly, many of the $5s5p5d$ and $5p^3$ levels are located above the first ionization limit. Therefore, only those levels that have autoionization rates comparable to or smaller than the radiative decay rate were observed via their corresponding photon decay channel.

Although, as noted above, some studies of the $4d$ core-excited spectrum of Sn II have been published [12, 13], we restrict the scope of this paper to excitations of the $n = 5$ electrons.

2. Experimental details

The tin ions/atoms were excited by means of a triggered spark source, which consists of a $14.5\ \mu\text{F}$ fast-charging low-inductance capacitor, chargeable up to 20 kV, and a trigger module to initiate the discharge. Either pure electrodes made of tin, or tin samples inserted into a cavity in aluminum electrodes were used. The tin spectrum was recorded at St. Francis Xavier University, Antigonish (Canada) using a 3 m normal incidence vacuum ultraviolet (VUV) spectrograph in the (300–2080) Å wavelength region. A holographic osmium-coated grating with 2400 lines/mm was used to obtain reciprocal linear dispersion of about $1.4\ \text{Å}/\text{mm}$ in the aforementioned region in the first order of diffraction. At least four or five different tracks of spectrum were photographed on a Kodak SWR¹ (short-wave radiation) plates with varied experimental conditions, such as electric current and voltage. The purpose of the different exposures was to distinguish the lines of Sn II from other ionization species. This was achieved by inserting a low, medium, or high inductance in series with the spark circuit or by varying the charging potential within the limits of 2 kV and 6 kV. The inductances were made of copper wire, 2 mm in diameter, wound on a cylinder of diameter 24 cm in turns separated by about 4 mm. A low inductance coil had 8 or 9 turns of wire, a medium one had 25 turns, and the high inductance one had 40 to 50 turns. The optimal conditions for observing the Sn II spectrum were found to be at 2 kV without an additional inductance or at 4 kV with a medium inductance. Relative positions of spectral lines on the plates were measured using a Zeiss Abbe¹ comparator at the Aligarh University (India). For their wavelength reduction, the known impurity lines of C, O, Al, and Si [18] were used as internal standards to obtain a second- or third-degree polynomial fit with a mean deviation of $0.005\ \text{Å}$ or less. This value represents the wavelength uncertainty

¹ Commercial products are identified in this paper for adequate specification of the experimental procedure. This identification does not imply recommendation or endorsement by NIST.

of our measurements for sharp and unperturbed lines. A more detailed discussion of uncertainties is given in the next section.

3. Measurement uncertainties

The general estimate of uncertainty given in the previous section, 0.005 Å for strong unperturbed lines, is insufficient for deriving accurate energy level values from the observed wavelengths. For that purpose, it is necessary to estimate the uncertainty for each individual line. We examined all our observed lines and assigned somewhat greater uncertainties to blended lines and those that appear to be broadened and/or asymmetric. The largest uncertainty, 0.010 Å, was assigned to blended and hazy lines. Many of the latter category lines appear to be broadened by autoionization of the upper level. The values of uncertainty assigned to each line can be found in table 1. All uncertainties reported in the present work are meant to be on the level of one standard deviation.

Many of the known classified lines of Sn II were observed by other researchers [6, 10, 11] outside the wavelength range studied in the present work. Thus, to obtain optimized level values, wavelength values and uncertainties reported by other observers have to be evaluated.

The most valuable of the previously reported measurements are those of Brill [10]. He reported 42 wavelengths of Sn II between 2150 Å and 10740 Å, with uncertainties estimated individually for each line. For 39 of these lines, the measurements were made interferometrically, and their uncertainties vary between 0.0006 Å and 0.006 Å. Three weak lines were measured with a grating spectrograph; their uncertainties are between 0.06 Å and 0.09 Å.

Two other large sets of wavelengths were taken from Wu's thesis [11] and from McCormick and Sawyer [6]. Wu photographed the tin spectra in the region between 350 Å and 9000 Å using an electrodeless discharge. A condensed spark in helium with a 3 m normal incidence vacuum grating spectrograph and a prism spectrograph were used in the regions below and above 2400 Å, respectively. Although all wavelengths in Wu's line list were given with three digits after the decimal point (in angstroms), the wavelength uncertainty varied greatly depending on the wavelength region and on the spectrographs used. To assess the uncertainties of Wu's wavelength measurements, we compared his reported wavelengths with more accurate ones taken from ASD [5] for Sn I and Sn III and with the Sn II Ritz wavelengths (see section 4) determined mainly by our measurements in the VUV and by Brill's measurements [10] in the air region. This comparison, shown in figures 1a, 1b, and 1c, revealed significant systematic shifts. These shifts vary smoothly with wavelength between +0.019 Å near 900 Å and -0.25 Å near 8300 Å. After removing these shifts, the measurement uncertainties of the corrected wavelengths were estimated from their average deviations from reference values. In the region below 2400 Å, where the grating spectrograph was used, the estimated wavelength uncertainty is almost constant, about 0.019 Å. In the region 2400 Å to 3050 Å, where the quartz prism spectrograph was used, the uncertainties are about 0.024 Å on average. However, uncertainties of Wu's prism spectra are better described by a constant uncertainty in wavenumber, about 0.3 cm⁻¹ for this wavelength region. This implies a gradual increase of uncertainties from 0.019 Å at 2400 Å to 0.03 Å at 3050 Å. Above this wavelength, as figure 1c shows, uncertainties increase abruptly to 1.7 cm⁻¹, corresponding to 0.16 Å at 3100 Å and 1.2 Å at 8300 Å.

McCormick and Sawyer [6] excited the Sn II spectrum in a hollow cathode discharge in helium and photographed it in a similarly wide wavelength range from 800 Å to 10 000 Å. In the region below 2200 Å, they used a 1 m vacuum grating spectrograph. The region from 2200 Å to 2700 Å was photographed with a quartz prism spectrograph. Above 2700 Å, two other prism spectrographs were used. Since these authors reported only the Sn II wavelengths, the only means of assessment of their uncertainties was a comparison with more accurate Ritz wavelengths. For this comparison, we used the Ritz wavelengths from our preliminary level optimization (see section 4) that were mainly determined by our VUV measurements and those of Brill [10] in the region above 2150 Å. Figure 1d shows these deviations, scaled in such a way that their scatter has similar magnitudes throughout the wavelength range covered by the figure.

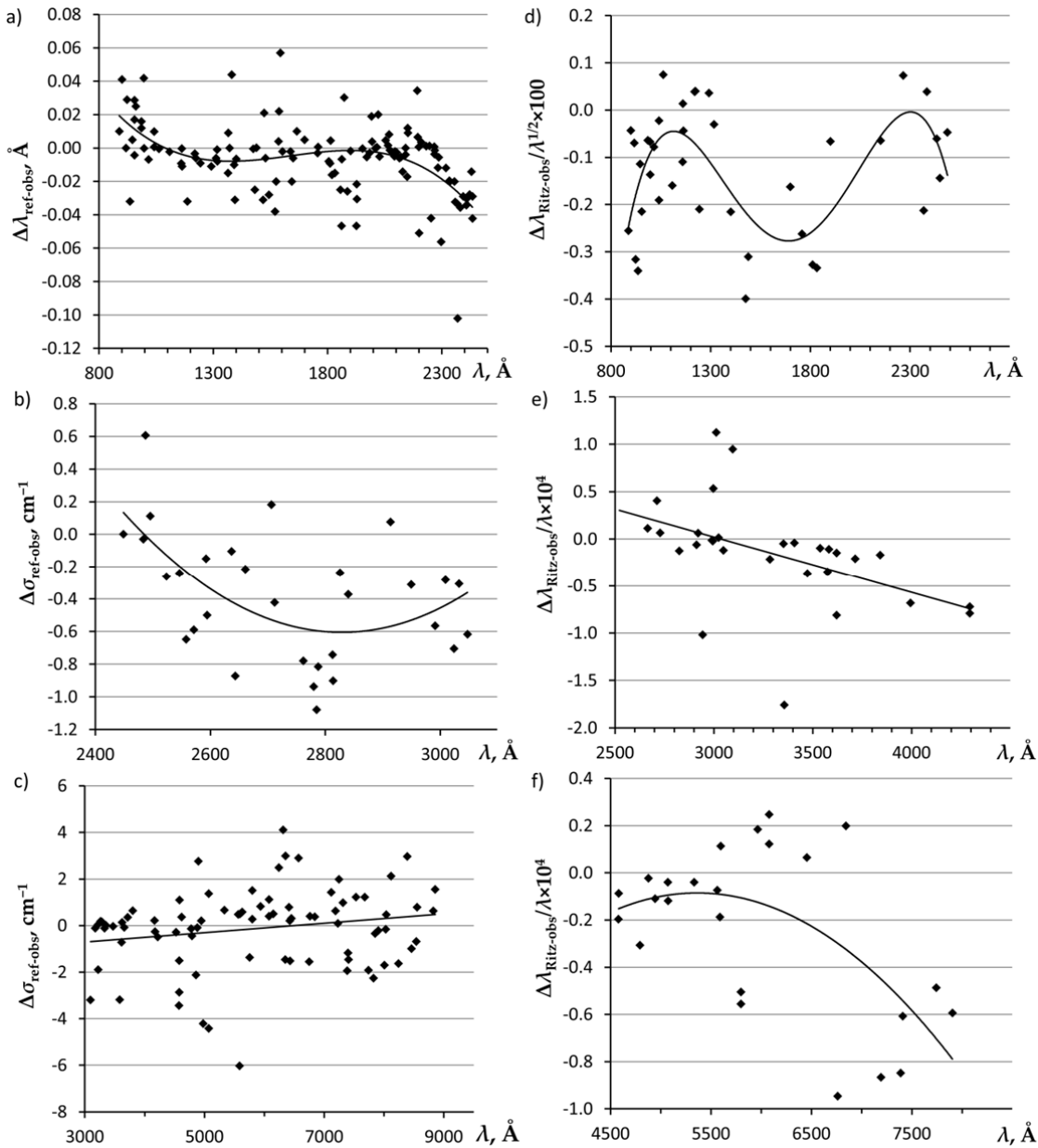


Figure 1. Differences between observed and reference wavelengths λ or wave numbers σ for the measurements of Wu [11] (a, b, c) and McCormick and Sawyer [6] (d, e, f). The solid lines are linear or polynomial fits determining the systematic corrections to the original measurements.

As with the work of Wu, measurements of McCormick and Sawyer [6] appear to have significant systematic shifts smoothly varying with wavelength, from -0.11 \AA at 1700 \AA to zero at 2300 \AA . At longer wavelengths, as figures 1e and 1f show, statistical uncertainties appear to be almost constant, if they are scaled by dividing them by wavelength. Systematic shifts are significant in these regions as well, varying from $+0.08 \text{ \AA}$ at about 3000 \AA to -0.6 \AA at 8000 \AA .

All identified lines of Sn II are collected in table 1 with the adopted wavelengths and their uncertainties. In total, there are about 200 lines, of which 70 were measured in the present work, 42 are from Brill [10], 27 are from McCormick and Sawyer [6], and 63 are from Wu [11]. Among Wu's lines [11], 12 were classified as Sn II transitions by us.

Table 1. Classified lines in Sn II

$I_{\text{obs}}^{\text{a}}$ arb. u.	Char. ^b	$\lambda_{\text{obs}}^{\text{c}}$ Å	$\sigma_{\text{obs}}^{\text{c}}$ cm ⁻¹	$\lambda_{\text{Ritz}}^{\text{d}}$ Å	$\delta\lambda_{\text{O-Ritz}}^{\text{e}}$ Å	Classification	$E_{\text{low}}^{\text{f}}$ cm ⁻¹	$E_{\text{upp}}^{\text{f}}$ cm ⁻¹	A^{f} s ⁻¹	Acc. ^g	Line Ref. ^h	TP Ref. ^h
1400		888.313(19)	112572.9	888.304(4)	0.009	5s ² 5p 2P ^o _{1/2} 5s ² 11d 2D _{3/2}	0.00	112574.1			Wu	
3400		899.884(19)	111125.4	899.907(10)	-0.023	5s ² 5p 2P ^o _{1/2} 5s ² 10d 2D _{3/2}	0.00	111122.6			Wu	
7300		917.378(5)	109006.3	917.379(3)	-0.001	5s ² 5p 2P ^o _{1/2} 5s ² 9d 2D _{3/2}	0.00	109006.2	9.+7	E	TW	TW
3500		922.856(19)	108359.3	922.870(3)	-0.014	5s ² 5p 2P ^o _{1/2} 5s ² 10s 2S _{1/2}	0.00	108357.6	2.4+7	E	Wu	TW
3700		923.01(4)	108341	922.974(10)	0.04	5s ² 5p 2P ^o _{3/2} 5s ² 11d 2D _{5/2}	4251.505	112596.9			MS	
5800		935.571(19)	106886.6	935.526(10)	0.045	5s ² 5p 2P ^o _{3/2} 5s ² 10d 2D _{5/2}	4251.505	111143.3			Wu	
14000		945.801(5)	105730.5	945.795(3)	0.006	5s ² 5p 2P ^o _{1/2} 5s ² 8d 2D _{3/2}	0.00	105731.2	1.5+8	E	TW	TW
12000		954.445(5)	104772.9	954.4337(14)	0.011	5s ² 5p 2P ^o _{3/2} 5s ² 9d 2D _{5/2}	4251.505	109025.68	9.+7	E	TW	TW
6200		954.612(5)	104754.6	954.611(3)	0.001	5s ² 5p 2P ^o _{3/2} 5s ² 9d 2D _{3/2}	4251.505	109006.2	1.8+7	E	TW	TW
6900		955.301(5)	104679.0	955.3066(10)	-0.006	5s ² 5p 2P ^o _{1/2} 5s ² 9s 2S _{1/2}	0.00	104678.43	3.9+7	E	TW	TW
2400		960.545(19)	104107.6	960.559(4)	-0.014	5s ² 5p 2P ^o _{3/2} 5s ² 10s 2S _{1/2}	4251.505	108357.6	4.+7	E	Wu	TW
18000		985.101(5)	101512.4	985.1099(22)	-0.009	5s ² 5p 2P ^o _{3/2} 5s ² 8d 2D _{5/2}	4251.505	105763.02	1.6+8	E	TW	TW
10000		985.411(19)	101480.5	985.419(3)	-0.008	5s ² 5p 2P ^o _{3/2} 5s ² 8d 2D _{3/2}	4251.505	105731.2	3.0+7	E	Wu	TW
8600		995.743(5)	100427.5	995.7489(10)	-0.006	5s ² 5p 2P ^o _{3/2} 5s ² 9s 2S _{1/2}	4251.505	104678.43	7.+7	E	TW	TW
19000		997.157(5)	100285.1	997.1668(5)	-0.010	5s ² 5p 2P ^o _{1/2} 5s ² 7d 2D _{3/2}	0.00	100284.125	2.8+8	D+	TW	TW
16000		1016.240(5)	98402.0	1016.2351(5)	0.005	5s ² 5p 2P ^o _{1/2} 5s ² 8s 2S _{1/2}	0.00	98402.425	7.+7	E	TW	TW
24000		1040.722(5)	96087.1	1040.71858(18)	0.003	5s ² 5p 2P ^o _{3/2} 5s ² 7d 2D _{5/2}	4251.505	100338.960	3.0+8	D+	TW	TW
16000		1041.315(5)	96032.4	1041.31284(19)	0.002	5s ² 5p 2P ^o _{3/2} 5s ² 7d 2D _{3/2}	4251.505	100284.125	6.+7	E	TW	TW
25000		1062.126(5)	94150.8	1062.12451(17)	0.001	5s ² 5p 2P ^o _{3/2} 5s ² 8s 2S _{1/2}	4251.505	98402.425	1.3+8	E	TW	TW
43000		1108.130(7)	90242.1	1108.1368(5)	-0.007	5s ² 5p 2P ^o _{1/2} 5s ² 6d 2D _{3/2}	0.00	90241.568	4.7+8	B+	TW	OH10
53000		1159.013(7)	86280.3	1159.0127(6)	0.000	5s ² 5p 2P ^o _{1/2} 5s ² 7s 2S _{1/2}	0.00	86280.332	1.01+8	C+	TW	OH10
74000		1161.427(7)	86101.0	1161.43475(20)	-0.008	5s ² 5p 2P ^o _{3/2} 5s ² 6d 2D _{5/2}	4251.505	90351.908	5.5+8	B+	TW	OH10
56000		1162.920(7)	85990.4	1162.92507(20)	-0.005	5s ² 5p 2P ^o _{3/2} 5s ² 6d 2D _{3/2}	4251.505	90241.568	1.28+8	B+	TW	OH10
37000		1185.679(10)	84339.9	1185.678(4)	0.001	5s5p ² 4P _{3/2} 5s5p(1P ^o)5d 2D ^o _{5/2}	48368.198	132708.1			TW	
66000	bl(Si II)	1193.289(10)	83802.0	1193.3067(24)	-0.018	5s5p ² 4P _{3/2} 5s5p(1P ^o)5d 2D ^o _{3/2}	48368.198	132168.95			TW	
91000		1219.083(7)	82028.9	1219.08363(22)	-0.001	5s ² 5p 2P ^o _{3/2} 5s ² 7s 2S _{1/2}	4251.505	86280.332	3.35+8	B+	TW	OH10
100000		1223.709(7)	81718.8	1223.714(4)	-0.005	5s ² 5p 2P ^o _{1/2} 5s5p ² 2P _{3/2}	0.00	81718.43	4.08+8	B+	TW	OH10
110000		1242.922(7)	80455.6	1242.926(5)	-0.004	5s ² 5p 2P ^o _{1/2} 5s5p ² 2P _{1/2}	0.00	80455.3	4.5+8	B+	TW	OH10
31000		1285.659(5)	77781.1	1285.653(3)	0.006	5s5p ² 4P _{1/2} 5s5p(3P ^o)5d 4P ^o _{3/2}	46464.301	124245.80			TW	
200000		1290.874(7)	77466.9	1290.873(4)	0.001	5s ² 5p 2P ^o _{3/2} 5s5p ² 2P _{3/2}	4251.505	81718.43	2.95+9	B+	TW	OH10
37000	H	1303.902(10)	76692.9	1303.908(5)	-0.006	5s5p ² 4P _{1/2} 5p3 4S ^o _{3/2}	46464.301	123156.8	9.+8	D+	TW	TW
210000		1312.273(7)	76203.7	1312.271(5)	0.002	5s ² 5p 2P ^o _{3/2} 5s5p ² 2P _{1/2}	4251.505	80455.3	1.77+9	B+	TW	OH10

$I_{\text{obs}}^{\text{a}}$ arb. u.	Char. ^b	$\lambda_{\text{obs}}^{\text{c}}$ Å	$\sigma_{\text{obs}}^{\text{c}}$ cm ⁻¹	$\lambda_{\text{Ritz}}^{\text{d}}$ Å	$\delta\lambda_{\text{O-Ritz}}^{\text{e}}$ Å	Classification	$E_{\text{low}}^{\text{f}}$ cm ⁻¹	$E_{\text{upp}}^{\text{f}}$ cm ⁻¹	A^{f} s ⁻¹	Acc. ^g	Line Ref. ^h	TP Ref. ^h
100000	bl(Sn III)	1313.090(10)	76156.2	1313.090(10)		5s5p ² 4P _{3/2} 5s5p(3P°)5d 4P° _{1/2}	48368.198	124524.4	2.0+9	D+	TW	TW
210000		1316.579(7)	75954.4	1316.579(5)	0.000	5s ² 5p 2P° _{1/2} 5s5p ² 2S _{1/2}	0.00	75954.4	2.14+9	B+	TW	OH10
86000		1317.906(5)	75877.9	1317.912(3)	-0.006	5s5p ² 4P _{3/2} 5s5p(3P°)5d 4P° _{3/2}	48368.198	124245.80	1.3+9	D+	TW	TW
33000	H	1327.668(10)	75320.0	1327.667(7)	0.001	5s5p ² 4P _{3/2} 5s5p(3P°)5d 4P° _{5/2}	48368.198	123688.3			TW	
67000	h	1337.102(10)	74788.6	1337.102(5)	0.000	5s5p ² 4P _{3/2} 5p3 4S° _{3/2}	48368.198	123156.8	1.3+9	D+	TW	TW
13000	H	1353.843(10)	73863.8	1353.841(5)	0.002	5s5p ² 2D _{3/2} 5s5p(1P°)5d 2D° _{5/2}	58844.194	132708.1	3.6+8	D+	TW	TW
58000	h	1358.705(10)	73599.5	1358.692(7)	0.013	5s5p ² 4P _{1/2} 5s5p(3P°)5d 4D° _{3/2}	46464.301	120064.5	1.9+9	D+	TW	TW
200000	H,bl(Sn III)*	1360.224(10)	73517.3	1360.256(3)	-0.032	5s5p ² 4P _{5/2} 5s5p(3P°)5d 4P° _{3/2}	50730.237	124245.80	7.5+8	D+	TW	TW
120000	H,bl(Sn III)*	1360.224(10)	73517.3	1360.230(8)	-0.006	5s5p ² 4P _{1/2} 5s5p(3P°)5d 4D° _{1/2}	46464.301	119981.3	3.3+9	D+	TW	TW
93000		1363.797(5)	73324.7	1363.796(3)	0.001	5s5p ² 2D _{3/2} 5s5p(1P°)5d 2D° _{3/2}	58844.194	132168.95	3.6+9	D+	TW	TW
100000	H	1365.278(10)	73245.2	1365.288(5)	-0.010	5s5p ² 2D _{5/2} 5s5p(1P°)5d 2D° _{5/2}	59463.494	132708.1	3.4+9	D+	TW	TW
100000	H,bl(Sn III)	1370.649(10)	72958.1	1370.650(7)	-0.001	5s5p ² 4P _{5/2} 5s5p(3P°)5d 4P° _{5/2}	50730.237	123688.3	2.1+9	D+	TW	TW
46000		1375.413(5)	72705.4	1375.413(3)	0.000	5s5p ² 2D _{5/2} 5s5p(1P°)5d 2D° _{3/2}	59463.494	132168.95	1.8+8	D+	TW	TW
68000	H	1380.701(10)	72427.0	1380.709(6)	-0.008	5s5p ² 4P _{5/2} 5p3 4S° _{3/2}	50730.237	123156.8	2.3+9	D+	TW	TW
130000	s	1391.097(7)	71885.7	1391.098(4)	-0.001	5s5p ² 4P _{3/2} 5s5p(3P°)5d 4D° _{5/2}	48368.198	120253.85	2.3+9	D+	TW	TW
130000	H	1393.507(10)	71761.4	1393.507(10)		5s5p ² 4P _{5/2} 5s5p(3P°)5d 4D° _{7/2}	50730.237	122491.6	3.1+9	D+	TW	TW
62000		1394.667(19)	71701.7	1394.644(5)	0.023	5s ² 5p 2P° _{3/2} 5s5p ² 2S _{1/2}	4251.505	75954.4	7.+6	E	Wu*	OH10
19000	H	1394.761(10)	71696.9	1394.772(7)	-0.011	5s5p ² 4P _{3/2} 5s5p(3P°)5d 4D° _{3/2}	48368.198	120064.5	1.0+9	D+	TW	TW
15000	H	1396.396(10)	71612.9	1396.393(8)	0.003	5s5p ² 4P _{3/2} 5s5p(3P°)5d 4D° _{1/2}	48368.198	119981.3	2.4+8	D+	TW	TW
360000		1400.448(10)	71405.7	1400.4395(9)	0.009	5s ² 5p 2P° _{1/2} 5s ² 5d 2D _{3/2}	0.00	71406.155	2.05+9	B+	TW	OH10
5000		1438.362(10)	69523.5	1438.360(5)	0.002	5s5p ² 4P _{5/2} 5s5p(3P°)5d 4D° _{5/2}	50730.237	120253.85			TW	
530000		1474.995(10)	67796.8	1474.9966(3)	-0.002	5s ² 5p 2P° _{3/2} 5s ² 5d 2D _{5/2}	4251.505	72048.273	1.95+9	B+	TW	OH10
15000		1481.739(5)	67488.27	1481.737(3)	0.002	5s5p ² 4P _{1/2} 5s5p(3P°)6s 2P° _{1/2}	46464.301	113952.66			TW	
79000		1489.094(10)	67154.9	1489.1002(4)	-0.006	5s ² 5p 2P° _{3/2} 5s ² 5d 2D _{3/2}	4251.505	71406.155	1.59+8	B+	TW	OH10
32000		1495.033(5)	66888.16	1495.033(5)		5s5p ² 4P _{3/2} 5s5p(3P°)5d 4F° _{5/2}	48368.198	115256.35	1.1+8	D+	TW	TW
33000		1517.957(5)	65878.02	1517.962(3)	-0.005	5s5p ² 4P _{3/2} 5s5p(3P°)6s 4P° _{5/2}	48368.198	114245.98	4.4+8	D+	TW	TW
24000	bl(Sn)	1522.210(10)	65694.0	1522.228(6)	-0.018	5s5p ² 4P _{5/2} 5s5p(3P°)5d 4F° _{7/2}	50730.237	116423.4	8.3+7	D+	TW	TW
15000	bl(Sn)	1527.860(10)	65451.0	1527.873(4)	-0.013	5s5p ² 4P _{3/2} 5s5p(3P°)5d 2D° _{5/2}	48368.198	113818.68			TW	
14000		1543.653(19)	64781.4	1543.631(4)	0.022	5s5p ² 2D _{5/2} 5s5p(3P°)5d 4P° _{3/2}	59463.494	124245.80			Wu*	
60000		1554.878(10)	64313.7	1554.882(3)	-0.004	5s5p ² 4P _{1/2} 5s5p(3P°)6s 4P° _{3/2}	46464.301	110777.85	4.0+8	D+	TW	TW
13000		1570.056(19)	63692.0	1570.024(7)	0.032	5s5p ² 2D _{5/2} 5p3 4S° _{3/2}	59463.494	123156.8			Wu*	
33000		1574.417(5)	63515.57	1574.413(4)	0.004	5s5p ² 4P _{5/2} 5s5p(3P°)6s 4P° _{5/2}	50730.237	114245.98	7.2+8	D+	TW	TW
14000	bl(Sn)	1585.063(10)	63089.0	1585.076(4)	-0.013	5s5p ² 4P _{5/2} 5s5p(3P°)5d 2D° _{5/2}	50730.237	113818.68	6.2+7	D+	TW	TW

$I_{\text{obs}}^{\text{a}}$ arb. u.	Char. ^b	$\lambda_{\text{obs}}^{\text{c}}$ Å	$\sigma_{\text{obs}}^{\text{c}}$ cm^{-1}	$\lambda_{\text{Ritz}}^{\text{d}}$ Å	$\delta\lambda_{\text{O-Ritz}}^{\text{e}}$ Å	Classification	$E_{\text{low}}^{\text{f}}$ cm^{-1}	$E_{\text{upp}}^{\text{f}}$ cm^{-1}	A^{f} s^{-1}	Acc. ^g	Line Ref. ^h	TP Ref. ^h
9200		1587.532(19)	62990.9	1587.560(5)	-0.028	$5s5p^2$ $4P_{1/2}$ $5s5p(^3P^{\circ})6s$ $4P^{\circ}_{1/2}$	46464.301	109454.05	1.5+8	D+	Wu	TW
15000	bl(Sn)	1593.418(10)	62758.2	1593.425(6)	-0.007	$5s5p^2$ $4P_{1/2}$ $5s^210p$ $2P^{\circ}_{1/2}$	46464.301	109222.18			TW	
16000		1602.313(5)	62409.78	1602.316(3)	-0.003	$5s5p^2$ $4P_{3/2}$ $5s5p(^3P^{\circ})6s$ $4P^{\circ}_{3/2}$	48368.198	110777.85	1.1+8	D+	TW	TW
22000	bl(Sn III)	1628.409(10)	61409.6	1628.408(6)	0.001	$5s5p^2$ $2D_{3/2}$ $5s5p(^3P^{\circ})5d$ $4D^{\circ}_{5/2}$	58844.194	120253.85			TW	
16000		1637.042(5)	61085.79	1637.040(5)	0.002	$5s5p^2$ $4P_{3/2}$ $5s5p(^3P^{\circ})6s$ $4P^{\circ}_{1/2}$	48368.198	109454.05	6.6+8	D+	TW	TW
8100		1643.294(10)	60853.4	1643.278(6)	0.016	$5s5p^2$ $4P_{3/2}$ $5s^210p$ $2P^{\circ}_{1/2}$	48368.198	109222.18	1.4+8	D+	TW	TW
6300		1648.545(10)	60659.6	1648.538(7)	0.007	$5s^25d$ $2D_{5/2}$ $5s5p(^1P^{\circ})5d$ $2D^{\circ}_{5/2}$	72048.273	132708.1			TW	
19000		1665.346(5)	60047.58	1665.345(3)	0.001	$5s5p^2$ $4P_{5/2}$ $5s5p(^3P^{\circ})6s$ $4P^{\circ}_{3/2}$	50730.237	110777.85	3.8+8	D+	TW	TW
21000		1699.403(10)	58844.2	1699.4030(13)	0.000	$5s^25p$ $2P^{\circ}_{1/2}$ $5s5p^2$ $2D_{3/2}$	0.00	58844.194	2.99+7	B+	TW	OH10
1700		1755.621(19)	56959.9	1755.621(8)	0.000	$5s5p^2$ $2D_{5/2}$ $5s5p(^3P^{\circ})5d$ $4F^{\circ}_{7/2}$	59463.494	116423.4			Wu*	
15000		1757.891(10)	56886.3	1757.8901(14)	0.001	$5s^25p$ $2P^{\circ}_{1/2}$ $5s^26s$ $2S_{1/2}$	0.00	56886.3763	3.04+8	B+	TW	OH10
6500	bl(Sn)	1778.904(10)	56214.4	1778.899(8)	0.005	$5s5p^2$ $2S_{1/2}$ $5s5p(^1P^{\circ})5d$ $2D^{\circ}_{3/2}$	75954.4	132168.95			TW	
1900		1805.002(19)	55401.6	1804.996(5)	0.006	$5s5p^2$ $2D_{3/2}$ $5s5p(^3P^{\circ})6s$ $4P^{\circ}_{5/2}$	58844.194	114245.98			Wu	
14000		1811.210(10)	55211.7	1811.2008(5)	0.009	$5s^25p$ $2P^{\circ}_{3/2}$ $5s5p^2$ $2D_{5/2}$	4251.505	59463.494	6.4+7	B+	TW	OH10
1100		1814.602(5)	55108.50	1814.603(4)	-0.001	$5s5p^2$ $2D_{3/2}$ $5s5p(^3P^{\circ})6s$ $2P^{\circ}_{1/2}$	58844.194	113952.66			TW	
1500		1819.045(10)	54973.9	1819.026(6)	0.019	$5s5p^2$ $2D_{3/2}$ $5s5p(^3P^{\circ})5d$ $2D^{\circ}_{5/2}$	58844.194	113818.68			TW	
11000		1831.727(10)	54593.3	1831.7471(5)	-0.020	$5s^25p$ $2P^{\circ}_{3/2}$ $5s5p^2$ $2D_{3/2}$	4251.505	58844.194	2.2+7	C+	TW	OH10
370		1855.604(19)	53890.8	1855.581(4)	0.023	$5s^26s$ $2S_{1/2}$ $5s5p(^3P^{\circ})6s$ $4P^{\circ}_{3/2}$	56886.3763	110777.85			Wu	
570		1886.142(19)	53018.3	1886.117(8)	0.025	$5s5p^2$ $4P_{3/2}$ $5s^28p$ $2P^{\circ}_{3/2}$	48368.198	101387.18			Wu	
7200		1899.890(10)	52634.6	1899.8812(5)	0.009	$5s^25p$ $2P^{\circ}_{3/2}$ $5s^26s$ $2S_{1/2}$	4251.505	56886.3763	5.6+8	B+	TW	OH10
170		2108.475(19)	47412.6	2108.493(12)	-0.018	$5s5p^2$ $2D_{3/2}$ $5s^29p$ $2P^{\circ}_{1/2}$	58844.194	106256.4			Wu	
250		2131.208(19)	46906.9	2131.219(18)	-0.011	$5s5p^2$ $2D_{5/2}$ $5s^29p$ $2P^{\circ}_{3/2}$	59463.494	106370.2			Wu	
720	bl(Sn III)	2148.61(8)	46527.1	2148.590(16)	0.02	$5s5p^2$ $2D_{3/2}$ $5s^26f$ $2F^{\circ}_{5/2}$	58844.194	105371.7			MS	
520		2150.8442(9)	46478.749	2150.8450(7)	-0.0008	$5s^25p$ $2P^{\circ}_{3/2}$ $5s5p^2$ $4P_{5/2}$	4251.505	50730.237	4.0+5	D+	Brill	OH10
530		2151.5135(20)	46464.29	2151.5131(19)	0.0004	$5s^25p$ $2P^{\circ}_{1/2}$ $5s5p^2$ $4P_{1/2}$	0.00	46464.301	2.1+6	C+	Brill	OH10
160		2200.075(19)	45438.8	2200.0340(11)	0.041	$5s5p^2$ $4P_{1/2}$ $5s^27p$ $2P^{\circ}_{1/2}$	46464.301	91903.958			Wu	
	m(Sn I)			2246.454(11)		$5s^26s$ $2S_{1/2}$ $5s^28p$ $2P^{\circ}_{3/2}$	56886.3763	101387.18			MS	
67		2252.845(19)	44374.6	2252.817(13)	0.028	$5s^25d$ $2D_{5/2}$ $5s5p(^3P^{\circ})5d$ $4F^{\circ}_{7/2}$	72048.273	116423.4			Wu*	
35		2255.726(19)	44317.9	2255.730(19)	-0.004	$5s^26s$ $2S_{1/2}$ $5s^28p$ $2P^{\circ}_{1/2}$	56886.3763	101204.2			Wu	
260		2266.0156(10)	44116.677	2266.0148(7)	0.0008	$5s^25p$ $2P^{\circ}_{3/2}$ $5s5p^2$ $4P_{3/2}$	4251.505	48368.198	4.3+5	D+	Brill	OH10
86		2296.293(19)	43535.0	2296.2548(9)	0.038	$5s5p^2$ $4P_{3/2}$ $5s^27p$ $2P^{\circ}_{1/2}$	48368.198	91903.958			Wu	
45		2333.43(14)	42842	2333.561(8)	-0.13	$5s^25d$ $2D_{3/2}$ $5s5p(^3P^{\circ})6s$ $4P^{\circ}_{5/2}$	71406.155	114245.98			Wu	
120		2349.825(19)	42543.3	2349.844(12)	-0.019	$5s5p^2$ $2D_{3/2}$ $5s^28p$ $2P^{\circ}_{3/2}$	58844.194	101387.18			Wu	

$I_{\text{obs}}^{\text{a}}$ arb. u.	Char. ^b	$\lambda_{\text{obs}}^{\text{c}}$ Å	$\sigma_{\text{obs}}^{\text{c}}$ cm ⁻¹	$\lambda_{\text{Ritz}}^{\text{d}}$ Å	$\delta\lambda_{\text{O-Ritz}}^{\text{e}}$ Å	Classification	$E_{\text{low}}^{\text{f}}$ cm ⁻¹	$E_{\text{upp}}^{\text{f}}$ cm ⁻¹	A^{f} s ⁻¹	Acc. ^g	Line Ref. ^h	TP Ref. ^h
130		2350.698(19)	42527.5	2350.707(14)	-0.009	5s5p ² 2P _{3/2} 5s5p(3P°)5d 4P° _{3/2}	81718.43	124245.80			Wu	
	m			2357.073(10)		5s ² 5d 2D _{3/2} 5s5p(3P°)5d 2D° _{5/2}	71406.155	113818.68			Wu	
	m			2359.996(21)		5s5p ² 2D _{3/2} 5s ² 8p 2P° _{1/2}	58844.194	101204.2			Wu	
3700		2360.28(10)	42355	2360.208(14)	0.07x	5s ² 6d 2D _{5/2} 5s5p(1P°)5d 2D° _{5/2}	90351.908	132708.1			Wu*	
310		2368.2265(6)	42212.795	2368.2265(6)	0.0000	5s ² 5p 2P° _{3/2} 5s5p ² 4P _{1/2}	4251.505	46464.301	5.6+5	C+	Brill	OH10
48		2369.15(10)	42196.4	2369.073(8)	0.08	5s ² 5d 2D _{5/2} 5s5p(3P°)6s 4P° _{5/2}	72048.273	114245.98			Wu	
220		2384.565(19)	41923.6	2384.559(12)	0.006	5s5p ² 2D _{5/2} 5s ² 8p 2P° _{3/2}	59463.494	101387.18			Wu	
53		2393.309(19)	41770.4	2393.310(10)	-0.001	5s ² 5d 2D _{5/2} 5s5p(3P°)5d 2D° _{5/2}	72048.273	113818.68			Wu*	
85		2406.712(19)	41537.8	2406.7088(6)	0.003	5s5p ² 4P _{5/2} 5s ² 7p 2P° _{3/2}	50730.237	92268.119	3.4+5	D+	Wu	OH10
160	bl(Sn I)	2433.48(3)	41080.9	2433.49(3)	-0.01	5s ² 6p 2P° _{1/2} 5s ² 11d 2D _{3/2}	71493.287	112574.1			Wu	
5700	:	2442.7	40926	2442.7019(6)		5s5p ² 4P _{3/2} 5s ² 4f 2F° _{5/2}	48368.198	89294.068	2.4+5	D+	AM	OH10
3500		2448.9079(7)	40822.163	2448.9089(4)	-0.0010	5s5p ² 2D _{3/2} 5s ² 5f 2F° _{5/2}	58844.194	99666.340	6.4+7	D+	Brill	TW
2300	:	2486.6	40203	2486.6356(5)		5s5p ² 2D _{5/2} 5s ² 5f 2F° _{5/2}	59463.494	99666.340	1.0+7	D	AM	AM
4100		2486.9666(8)	40197.495	2486.9665(4)	0.0001	5s5p ² 2D _{5/2} 5s ² 5f 2F° _{7/2}	59463.494	99660.991	6.8+7	D+	Brill	TW
1700		2522.69(9)	39628.3	2522.63(8)	0.06	5s ² 6p 2P° _{1/2} 5s ² 10d 2D _{3/2}	71493.287	111122.6			MS	
1900		2538.95(10)	39374.5	2539.133(8)	-0.18x	5s ² 5d 2D _{3/2} 5s5p(3P°)6s 4P° _{3/2}	71406.155	110777.85			Wu	
190		2579.15(23)	38761	2578.82(7)	0.33	5s ² 6p 2P° _{3/2} 5s ² 10d 2D _{5/2}	72377.4616	111143.3	1.0+7	D+	MS	TW
550	:	2592.3	38564	2592.3281(5)		5s5p ² 4P _{5/2} 5s ² 4f 2F° _{5/2}	50730.237	89294.068	1.9+5	D+	AM	OH10
1200		2592.7198(17)	38558.01	2592.7181(5)	0.0017	5s5p ² 4P _{5/2} 5s ² 4f 2F° _{7/2}	50730.237	89288.268	2.9+6	C+	Brill	OH10
200		2608.74(24)	38321	2608.74(24)		5s ² 6p 2P° _{3/2} 5s ² 11s 2S _{1/2}	72377.4616	110699			MS	
880	bl(Sn III)	2643.56(3)	37816.5	2643.594(16)	-0.03	5s ² 5d 2D _{3/2} 5s ² 10p 2P° _{1/2}	71406.155	109222.18			Wu	
860		2664.99(10)	37512.4	2664.96(3)	0.03	5s ² 6p 2P° _{1/2} 5s ² 9d 2D _{3/2}	71493.287	109006.2	1.4+7	D+	MS	TW
220		2711.86(3)	36864.2	2711.85(3)	0.01	5s ² 6p 2P° _{1/2} 5s ² 10s 2S _{1/2}	71493.287	108357.6			Wu	
400		2727.76(3)	36649.3	2727.838(11)	-0.08	5s ² 6p 2P° _{3/2} 5s ² 9d 2D _{5/2}	72377.4616	109025.68	1.6+7	D+	Wu	TW
180		2778.4(3)	35982	2778.49(3)	-0.1	5s ² 6p 2P° _{3/2} 5s ² 10s 2S _{1/2}	72377.4616	108357.6			MS	
240		2825.51(3)	35381.4	2825.4849(7)	0.03	5s ² 6s 2S _{1/2} 5s ² 7p 2P° _{3/2}	56886.3763	92268.119	1.11+6	C+	Wu	OH10
210		2868.61(3)	34849.9	2868.578(23)	0.03	5s ² 5d 2D _{3/2} 5s ² 9p 2P° _{1/2}	71406.155	106256.4			Wu	
220		2912.82(10)	34320.9	2912.74(3)	0.08	5s ² 5d 2D _{5/2} 5s ² 9p 2P° _{3/2}	72048.273	106370.2			MS	
610		2919.86(3)	34238.2	2919.884(25)	-0.02	5s ² 6p 2P° _{1/2} 5s ² 8d 2D _{3/2}	71493.287	105731.2	2.4+7	D+	Wu	TW
190		2943.30(3)	33965.5	2943.30(3)	0.00	5s ² 5d 2D _{3/2} 5s ² 6f 2F° _{5/2}	71406.155	105371.7			Wu	
400		2949.54(3)	33893.7	2949.522(14)	0.02	5s ² 6d 2D _{5/2} 5s5p(3P°)5d 4P° _{3/2}	90351.908	124245.80			Wu	
220		2990.99(3)	33424.0	2990.9965(8)	-0.01	5s5p ² 2D _{3/2} 5s ² 7p 2P° _{3/2}	58844.194	92268.119	9.1+5	C+	Wu	OH10
790		2994.46(3)	33385.3	2994.434(20)	0.03	5s ² 6p 2P° _{3/2} 5s ² 8d 2D _{5/2}	72377.4616	105763.02	2.7+7	D+	Wu	TW

$I_{\text{obs}}^{\text{a}}$ arb. u.	Char. ^b	$\lambda_{\text{obs}}^{\text{c}}$ Å	$\sigma_{\text{obs}}^{\text{c}}$ cm ⁻¹	$\lambda_{\text{Ritz}}^{\text{d}}$ Å	$\delta\lambda_{\text{O-Ritz}}^{\text{e}}$ Å	Classification	$E_{\text{low}}^{\text{f}}$ cm ⁻¹	$E_{\text{upp}}^{\text{f}}$ cm ⁻¹	A^{f} s ⁻¹	Acc. ^g	Line Ref. ^h	TP Ref. ^h
110		2997.1(3)	33355	2997.29(3)	-0.2	5s ² 6p 2P ^o _{3/2} 5s ² 8d 2D _{3/2}	72377.4616	105731.2			MS	
260		3012.41(5)	33186.3	3012.519(9)	-0.11	5s ² 6p 2P ^o _{1/2} 5s ² 9s 2S _{1/2}	71493.287	104678.43			Wu	
450		3023.92(3)	33060.1	3023.9444(14)	-0.02	5s5p ² 2D _{3/2} 5s ² 7p 2P ^o _{1/2}	58844.194	91903.958	7.8+6	C+	Wu	OH10
680		3047.44(3)	32804.9	3047.4642(9)	-0.02	5s5p ² 2D _{5/2} 5s ² 7p 2P ^o _{3/2}	59463.494	92268.119	6.8+6	B+	Wu	OH10
930		3094.68(11)	32304.1	3094.984(9)	-0.30	5s ² 6p 2P ^o _{3/2} 5s ² 9s 2S _{1/2}	72377.4616	104678.43			MS	
480		3101.25(16)	32235.7	3101.39(3)	-0.14x	5s5p ² 2P _{3/2} 5s5p(3P ^o)6s 2P ^o _{1/2}	81718.43	113952.66			Wu*	
15000		3283.1399(9)	30449.874	3283.1399(7)	0.0000	5s5p ² 2D _{3/2} 5s ² 4f 2F ^o _{5/2}	58844.194	89294.068	1.70+8	B+	Brill	OH10
13000	:	3351.3	29830.6	3351.3021(8)		5s5p ² 2D _{5/2} 5s ² 4f 2F ^o _{5/2}	59463.494	89294.068	1.21+7	B+	AM	OH10
13000		3351.9523(12)	29824.788	3351.9538(8)	-0.0015	5s5p ² 2D _{5/2} 5s ² 4f 2F ^o _{7/2}	59463.494	89288.268	1.82+8	B+	Brill	OH10
87		3355.5(3)	29793	3354.96(4)	0.5	5s ² 5d 2D _{3/2} 5s ² 8p 2P ^o _{1/2}	71406.155	101204.2			MS	
350		3407.41(12)	29339.4	3407.466(25)	-0.06	5s ² 5d 2D _{5/2} 5s ² 8p 2P ^o _{3/2}	72048.273	101387.18			MS	
1700		3472.333(3)	28790.837	3472.3329(12)	0.000	5s ² 6p 2P ^o _{1/2} 5s ² 7d 2D _{3/2}	71493.287	100284.125	4.5+7	D+	Brill	TW
660		3537.47(13)	28260.7	3537.5363(12)	-0.07	5s ² 5d 2D _{3/2} 5s ² 5f 2F ^o _{5/2}	71406.155	99666.340	3.6+6	D	MS	AM
2100		3575.3255(12)	27961.499	3575.3255(12)	0.0000	5s ² 6p 2P ^o _{3/2} 5s ² 7d 2D _{5/2}	72377.4616	100338.960	5.0+7	D+	Brill	TW
440		3582.3511(14)	27906.663	3582.3510(13)	0.0001	5s ² 6p 2P ^o _{3/2} 5s ² 7d 2D _{3/2}	72377.4616	100284.125	8.3+6	D+	Brill	TW
110		3612.68(22)	27672.4	3612.688(16)	-0.01	5s ² 7s 2S _{1/2} 5s5p(3P ^o)6s 2P ^o _{1/2}	86280.332	113952.66			Wu*	
240		3619.96(13)	27616.7	3619.7860(12)	0.17	5s ² 5d 2D _{5/2} 5s ² 5f 2F ^o _{5/2}	72048.273	99666.340	6.2+6	D	MS	AM
530		3620.4854(15)	27612.732	3620.4872(10)	-0.0018	5s ² 5d 2D _{5/2} 5s ² 5f 2F ^o _{7/2}	72048.273	99660.991	2.0+6	E	Brill	M79
500		3715.1524(11)	26909.141	3715.1529(9)	-0.0005	5s ² 6p 2P ^o _{1/2} 5s ² 8s 2S _{1/2}	71493.287	98402.425	1.6+7	D+	Brill	TW
440		3841.3756(14)	26024.959	3841.3750(9)	0.0006	5s ² 6p 2P ^o _{3/2} 5s ² 8s 2S _{1/2}	72377.4616	98402.425	2.9+7	D+	Brill	TW
190	*	3984.6(4)	25089.8	3984.6(4)		5s ² 4f 2F ^o _{7/2} 5s ² 11g 2G _{9/2}	89288.268	114378.1	2.4+6	D+	MS	TW
190	*	3984.6(4)	25089.8	3984.6(4)		5s ² 4f 2F ^o _{7/2} 5s ² 11g 2G _{7/2}	89288.268	114378.1	8.+4	E	MS	TW
17		3994.3(4)	25028.7	3994.238(3)	0.1	5s5p ² 4P _{1/2} 5s ² 6p 2P ^o _{1/2}	46464.301	71493.287			MS	
180	*	4110.3(4)	24322.6	4110.3(3)	0.0	5s ² 4f 2F ^o _{7/2} 5s ² 10g 2G _{9/2}	89288.268	113610.5	3.4+6	D+	MS	TW
180	*	4110.3(4)	24322.6	4110.3(3)	0.0	5s ² 4f 2F ^o _{7/2} 5s ² 10g 2G _{7/2}	89288.268	113610.5	1.2+5	E	MS	TW
180		4111.3(4)	24316.2	4111.3(3)	0.0	5s ² 4f 2F ^o _{5/2} 5s ² 10g 2G _{7/2}	89294.068	113610.5	3.3+6	D+	MS	TW
28		4164.8(3)	24004.0	4164.727(25)	0.1	5s ² 6d 2D _{3/2} 5s5p(3P ^o)6s 4P ^o _{5/2}	90241.568	114245.98			Wu	
31		4172.2(3)	23961.4	4172.15(3)	0.1	5s ² 7d 2D _{3/2} 5s5p(3P ^o)5d 4P ^o _{3/2}	100284.125	124245.80			Wu	
36	bl(Sn IV)	4216.2(6)	23711	4216.248(22)	0.0	5s ² 6d 2D _{3/2} 5s5p(3P ^o)6s 2P ^o _{1/2}	90241.568	113952.66			Wu*	
170	*	4293.3(4)	23285.6	4293.27(14)	0.0	5s ² 4f 2F ^o _{7/2} 5s ² 9g 2G _{9/2}	89288.268	112574.0	5.1+6	D+	MS	TW
170	*	4293.3(4)	23285.6	4293.27(14)	0.0	5s ² 4f 2F ^o _{7/2} 5s ² 9g 2G _{7/2}	89288.268	112574.0	1.8+5	E	MS	TW
340		4294.33(15)	23280.0	4294.34(14)	-0.01	5s ² 4f 2F ^o _{5/2} 5s ² 9g 2G _{7/2}	89294.068	112574.0	4.9+6	D+	MS	TW
6		4323.0925(13)	23125.086	4323.0920(13)	0.0005	5s5p ² 4P _{3/2} 5s ² 6p 2P ^o _{1/2}	48368.198	71493.287	7.0+4	D+	Brill	OH10

$I_{\text{obs}}^{\text{a}}$ arb. u.	Char. ^b	$\lambda_{\text{obs}}^{\text{c}}$ Å	$\sigma_{\text{obs}}^{\text{c}}$ cm ⁻¹	$\lambda_{\text{Ritz}}^{\text{d}}$ Å	$\delta\lambda_{\text{O-Ritz}}^{\text{e}}$ Å	Classification	$E_{\text{low}}^{\text{f}}$ cm ⁻¹	$E_{\text{upp}}^{\text{f}}$ cm ⁻¹	A^{f} s ⁻¹	Acc. ^g	Line Ref. ^h	TP Ref. ^h
120		4573.7(4)	21858.0	4574.32(23)	-0.6	5s ² 4f 2F ^o _{7/2} 5s ² 10d 2D _{5/2}	89288.268	111143.3			Wu	
91		4575.0(4)	21851.8	4575.54(23)	-0.5	5s ² 4f 2F ^o _{5/2} 5s ² 10d 2D _{5/2}	89294.068	111143.3			Wu	
	m			4579.9(3)		5s ² 4f 2F ^o _{5/2} 5s ² 10d 2D _{3/2}	89294.068	111122.6			Wu	
150	*	4579.06(13)	21832.4	4579.04(9)	0.02	5s ² 4f 2F ^o _{7/2} 5s ² 8g 2G _{9/2}	89288.268	111120.8	8.0+6	D+	MS	TW
150	*	4579.06(13)	21832.4	4579.04(9)	0.02	5s ² 4f 2F ^o _{7/2} 5s ² 8g 2G _{7/2}	89288.268	111120.8	2.9+5	E	MS	TW
140		4580.22(13)	21826.9	4580.25(9)	-0.03	5s ² 4f 2F ^o _{5/2} 5s ² 8g 2G _{7/2}	89294.068	111120.8	7.7+6	D+	MS	TW
90		4618.2359(10)	21647.226	4618.2363(10)	-0.0004	5s5p ² 4P _{5/2} 5s ² 6p 2P ^o _{3/2}	50730.237	72377.4616	6.4+5	C+	Brill	OH10
48		4776.1(4)	20931.7	4776.07(8)	0.0	5s5p ² 2P _{1/2} 5s ² 8p 2P ^o _{3/2}	80455.3	101387.18			Wu	
62	h	4792.0732(19)	20861.963	4792.0730(15)	0.0002	5s ² 5d 2D _{3/2} 5s ² 7p 2P ^o _{3/2}	71406.155	92268.119	4.0+5	C+	Brill	OH10
100		4877.209(3)	20497.805	4877.209(3)	0.000	5s ² 5d 2D _{3/2} 5s ² 7p 2P ^o _{1/2}	71406.155	91903.958	5.6+6	B+	Brill	OH10
66		4895.1(4)	20422.9	4894.37(3)	0.7	5s ² 6d 2D _{5/2} 5s5p(3P ^o)6s 4P _{3/2}	90351.908	110777.85			Wu	
83		4917.1(4)	20331.5	4917.8(3)	-0.7	5s ² 7p 2P ^o _{3/2} 5s ² 11d 2D _{5/2}	92268.119	112596.9	3.4+6	D+	Wu	TW
150		4944.2562(20)	20219.846	4944.2561(16)	0.0001	5s ² 5d 2D _{5/2} 5s ² 7p 2P ^o _{3/2}	72048.273	92268.119	4.9+6	B+	Brill	OH10
360	*	5071.09(15)	19714.1	5071.12(11)	-0.03	5s ² 4f 2F ^o _{7/2} 5s ² 7g 2G _{9/2}	89288.268	109002.3	1.4+7	D+	MS	TW
360	*	5071.09(15)	19714.1	5071.12(11)	-0.03	5s ² 4f 2F ^o _{7/2} 5s ² 7g 2G _{7/2}	89288.268	109002.3	5.+5	E	MS	TW
	m			5071.60(10)		5s ² 4f 2F ^o _{5/2} 5s ² 9d 2D _{3/2}	89294.068	109006.2			Wu	
360		5072.62(15)	19708.2	5072.61(11)	0.01	5s ² 4f 2F ^o _{5/2} 5s ² 7g 2G _{7/2}	89294.068	109002.3	1.3+7	D+	MS	TW
1600		5332.3391(16)	18748.281	5332.3391(11)	0.0000	5s ² 6p 2P ^o _{1/2} 5s ² 6d 2D _{3/2}	71493.287	90241.568	9.9+7	B+	Brill	OH10
2700		5561.9101(16)	17974.443	5561.9091(15)	0.0010	5s ² 6p 2P ^o _{3/2} 5s ² 6d 2D _{5/2}	72377.4616	90351.908	1.13+8	B+	Brill	OH10
2600		5588.8152(18)	17887.913	5588.8153(16)	-0.0001	5s ² 5d 2D _{3/2} 5s ² 4f 2F ^o _{5/2}	71406.155	89294.068	7.8+7	B+	Brill	OH10
530	h	5596.2644(15)	17864.103	5596.2634(12)	0.0010	5s ² 6p 2P ^o _{3/2} 5s ² 6d 2D _{3/2}	72377.4616	90241.568	1.91+7	B+	Brill	OH10
490		5796.9078(15)	17245.794	5796.9075(13)	0.0003	5s ² 5d 2D _{5/2} 5s ² 4f 2F ^o _{5/2}	72048.273	89294.068	5.1+6	B+	Brill	OH10
2700		5798.860(3)	17239.988	5798.8578(18)	0.002	5s ² 5d 2D _{5/2} 5s ² 4f 2F ^o _{7/2}	72048.273	89288.268	7.7+7	B+	Brill	OH10
470	H	5965.84(6)	16757.46	5965.80(5)	0.04	5s ² 7p 2P ^o _{3/2} 5s ² 9d 2D _{5/2}	92268.119	109025.68	7.6+6	D+	Brill	TW
1500	*	6077.6331(19)	16449.220	6077.6304(16)	0.0027	5s ² 4f 2F ^o _{7/2} 5s ² 6g 2G _{9/2}	89288.268	105737.495	2.7+7	D+	Brill	TW
1500	*	6077.6331(19)	16449.220	6077.6304(16)	0.0027	5s ² 4f 2F ^o _{7/2} 5s ² 6g 2G _{7/2}	89288.268	105737.495	1.0+6	D+	Brill	TW
1400		6079.7696(24)	16443.439	6079.7742(18)	-0.0046	5s ² 4f 2F ^o _{5/2} 5s ² 6g 2G _{7/2}	89294.068	105737.495	2.6+7	D+	Brill	TW
380		6242.1(7)	16015.8	6241.14(15)	1.0	5s ² 6d 2D _{5/2} 5s ² 9p 2P ^o _{3/2}	90351.908	106370.2			Wu	
760		6428.4(7)	15551.7	6428.99(5)	-0.6	5s ² 8s 2S _{1/2} 5s5p(3P ^o)6s 2P ^o _{1/2}	98402.425	113952.66			Wu*	
2500		6453.5422(12)	15491.085	6453.5421(11)	0.0001	5s ² 6s 2S _{1/2} 5s ² 6p 2P ^o _{3/2}	56886.3763	72377.4616	7.0+7	B+	Brill	OH10
830		6569.7(7)	15217.2	6568.44(9)	1.3	5s ² 9d 2D _{5/2} 5s5p(3P ^o)5d 4P _{3/2}	109025.68	124245.80			Wu	
1000		6661.1(8)	15008.4	6661.1(8)		5s ² 6d 2D _{5/2} 5s ² 6f 2F ^o _{7/2}	90351.908	105360.3	1.6+7	D+	Wu	TW
840		6760.812(3)	14787.041	6760.8103(22)	0.002	5s ² 6p 2P ^o _{1/2} 5s ² 7s 2S _{1/2}	71493.287	86280.332	3.82+7	B+	Brill	OH10

$I_{\text{obs}}^{\text{a}}$ arb. u.	Char. ^b	$\lambda_{\text{obs}}^{\text{c}}$ Å	$\sigma_{\text{obs}}^{\text{c}}$ cm ⁻¹	$\lambda_{\text{Ritz}}^{\text{d}}$ Å	$\delta\lambda_{\text{O-Ritz}}^{\text{e}}$ Å	Classification	$E_{\text{low}}^{\text{f}}$ cm ⁻¹	$E_{\text{upp}}^{\text{f}}$ cm ⁻¹	A^{f} s ⁻¹	Acc. ^g	Line Ref. ^h	TP Ref. ^h
1300		6844.1859(20)	14606.911	6844.1860(15)	-0.0001	5s ² 6s 2S _{1/2} 5s ² 6p 2P ^o _{1/2}	56886.3763	71493.287	6.0+7	B+	Brill	OH10
1100		7190.776(3)	13902.873	7190.7774(24)	-0.001	5s ² 6p 2P ^o _{3/2} 5s ² 7s 2S _{1/2}	72377.4616	86280.332	7.2+7	B+	Brill	OH10
670		7230.1(9)	13827.3	7230.11(15)	0.0	5s ² 7p 2P ^o _{1/2} 5s ² 8d 2D _{3/2}	91903.958	105731.2	1.2+7	D+	Wu	TW
500		7314.5(9)	13667.7	7314.06(7)	0.4	5s ² 7d 2D _{3/2} 5s5p(3P ^o)6s 2P ^o _{1/2}	100284.125	113952.66			Wu*	
480		7387.1651(24)	13533.265	7387.1636(19)	0.0015	5s5p ² 2D _{3/2} 5s ² 6p 2P ^o _{3/2}	58844.194	72377.4616	2.27+6	B+	Brill	OH10
380		7408.22(21)	13494.8	7408.17(12)	0.05	5s ² 7p 2P ^o _{3/2} 5s ² 8d 2D _{5/2}	92268.119	105763.02	1.3+7	D+	MS	TW
450		7729.6(10)	12933.7	7728.3(7)	1.3	5s ² 5f 2F ^o _{7/2} 5s ² 11d 2D _{5/2}	99660.991	112596.9			Wu	
500		7741.425(3)	12913.965	7741.423(3)	0.002	5s5p ² 2D _{5/2} 5s ² 6p 2P ^o _{3/2}	59463.494	72377.4616	1.89+7	B+	Brill	OH10
	m			7745.1(3)		5s ² 5f 2F ^o _{5/2} 5s ² 11d 2D _{3/2}	99666.340	112574.1			Wu	
190		7825.97(9)	12774.45	7825.96(6)	0.01	5s ² 7p 2P ^o _{1/2} 5s ² 9s 2S _{1/2}	91903.958	104678.43	4.7+6	D+	Brill	TW
280		7903.532(4)	12649.091	7903.531(3)	0.001	5s5p ² 2D _{3/2} 5s ² 6p 2P ^o _{1/2}	58844.194	71493.287	1.96+7	B+	Brill	OH10
53		8055.72(9)	12410.13	8055.60(6)	0.12	5s ² 7p 2P ^o _{3/2} 5s ² 9s 2S _{1/2}	92268.119	104678.43	8.6+6	D+	Brill	TW
2600	*	9058.880(4)	11035.863	9058.886(3)	-0.006	5s ² 4f 2F ^o _{7/2} 5s ² 5g 2G _{9/2}	89288.268	100324.124	6.8+7	D+	Brill	TW
2600	*	9058.880(4)	11035.863	9058.886(3)	-0.006	5s ² 4f 2F ^o _{7/2} 5s ² 5g 2G _{7/2}	89288.268	100324.124	2.4+6	D+	Brill	TW
2200		9063.658(5)	11030.045	9063.649(4)	0.009	5s ² 4f 2F ^o _{5/2} 5s ² 5g 2G _{7/2}	89294.068	100324.124	6.5+7	D+	Brill	TW
1300		10607.434(6)	9424.768	10607.430(6)	0.004	5s ² 6d 2D _{3/2} 5s ² 5f 2F ^o _{5/2}	90241.568	99666.340	4.9+7	D+	Brill	TW
1200		10739.257(6)	9309.081	10739.255(5)	0.002	5s ² 6d 2D _{5/2} 5s ² 5f 2F ^o _{7/2}	90351.908	99660.991	5.1+7	D+	Brill	TW
				23521.08(23)		5s ² 5p 2P ^o _{1/2} 5s ² 5p 2P ^o _{3/2}	0.00	4251.505	6.94-1	M1 A+		B95

^a Observed relative intensities, in terms of total energy flux under the line profile, are reduced to a common arbitrary scale corresponding to a plasma in local thermodynamic equilibrium with an effective excitation temperature of 4.2 eV. These conditions correspond to exposure 1 of the experiment of Wu [11] (see section 4.4).

^b Character of observed line: bl – blended by a close line (the blending spectrum is indicated in parentheses); h – hazy line; H – very hazy line; s – asymmetric line extending towards shorter wavelengths; * – intensity shared by two or more transitions; m – masked by a stronger neighboring line (no wavelength measured); : – the wavelength was not measured (the value in λ_{obs} is a rounded Ritz wavelength).

^c Observed and Ritz wavelengths are given in standard air for wavenumbers σ between 5000 cm⁻¹ and 50000 cm⁻¹ and in vacuum outside of this range. The uncertainty (standard deviation) in the last digit is given in parentheses.

^d Ritz wavelengths and their uncertainties were determined in the least-squares level optimization procedure (see section 4.3).

^e Difference between observed and Ritz wavelength. If this column is blank, and λ_{obs} is not blank, this line alone determines one of the levels involved in the assigned transition. An “x” after the value indicates that this line was excluded from the level optimization.

^f In the transition probability values, the number after the “+” or “-” symbol means the power of 10.

^g Transition probability accuracy code is explained in table 6.

^h References to observed wavelengths and transition probabilities: AM – Alonso-Medina and Colón 2000 [34]; B95 – Biémont et al. 1995 [35]; Brill – Brill 1964 [11]; M79 – Miller et al. 1979 [39]; MS – McCormick and Sawyer 1938 [6]; OH10 – Oliver and Hibbert 2010 [14]; Wu – Wu 1967 [11]; Wu* – line measured by Wu [11] with our new or revised classification; TW – this work.

4. Results and discussion

4.1. Theoretical calculations

The theoretical calculation for energy levels, wavelengths, and transition probabilities of Sn II was made with Cowan's codes [19], which implement the Hartree–Fock (HF) method with perturbative account for relativistic and configuration-interaction (CI) effects. For the even parity system, the configurations included were $5s5p^2$, $5s^2ns$ ($n = 6-12$), $5s^2nd$ ($n = 5-12$), $5s^2ng$ ($n = 5-12$), $4f5s5p$, and $5s5d^2$; the odd parity set included $5s^2np$ ($n = 6-20$), $5s^2nf$ ($n = 4-20$), $5p^3$, $5s5p5d$, $5s5p6s$, $4f5s5d$, $4f5p^2$, and $5p5d^2$ configurations. The initial scaling of the Slater parameters was 100 % of the HF values for E_{av} and ζ_{nl} , while the F^k , G^k , and the CI parameters were scaled to 80 % of the HF values. Then the Slater parameters were varied in the least-squares fitting (LSF) procedure minimizing discrepancies between calculated and observed level values.

In the parametric fitting, the energy level calculations for even parity converged with a standard deviation of 77 cm^{-1} , while the odd-parity configurations were fitted with a standard deviation of 156 cm^{-1} . Transition probabilities and autoionization rates were calculated with wavefunctions modified according to the fitted parameters.

4.2. Analysis of the spectrum

4.2.1. The $5s^25p - [5s^2(ns+nd) + 5s5p^2]$ transition array

Excitation of the outer electron from the $5s^25p \ ^2P^o$ ground term leads to the $5s^2ns \ ^2S_{1/2}$ and $5s^2nd \ ^2D_{3/2,5/2}$ level series showing a simple doublet structure. The transitions from $5s^2ns \ ^2S_{1/2}$ ($n = 6-8$) to both levels of the ground term and those from $5s^29s$ to $5s^25p \ ^2P^o_{3/2}$ were already reported by McCormick and Sawyer [6]. The energy levels derived from their wavelengths were later improved by Shenstone and reported in AEL [4]. All these transitions are confirmed in our measurements with improved accuracy. McCormick and Sawyer [6] established the levels of $5s^210s$ and $11s$ by observing transitions to the $5s^26p$ levels in the air wavelength region. We were able to observe both transitions from $5s^29s$ to the levels of $5s^25p$ at 955.289 \AA ($\ ^2S_{1/2} \rightarrow \ ^2P^o_{1/2}$) and 995.738 \AA ($\ ^2S_{1/2} \rightarrow \ ^2P^o_{3/2}$). Wu [11] observed both transitions from $5s^210s$ to the ground-term levels. Other transitions from $5s^2ns$ ($n = 7-11$) to the $5s^2np$ ($n = 6-7$) levels have also been observed by us and by other researchers [6, 10, 11]. Thus, the levels of the $5s^2ns$ ($n = 6-11$) configurations are well established. They are the least perturbed, showing the leading *LS* percentages of their composition above 99 %. Our least-squares parametric fitting shows a good regularity and confirms all their identifications.

The $5s^2nd$ configurations were also listed in AEL [4]. We confirmed the levels of $5s^2nd$ ($n = 5-9$) with lines observed on our plates. Wu's identifications of transitions from the $5s^210d$ and $11d$ configurations [11] are also confirmed. Some additional transitions between the $5s^2np$ ($n = 6-8$) and $5s^2nd$ levels have also been observed (see table 1). It is important to mention here that there is a strong interaction between the $5s^25d$ and $5s5p^2$ configurations. For this reason, the $\ ^2D_{3/2,5/2}$ levels of these configurations are strongly mixed each other. This strong mixing was indicated by relativistic CI calculations of Oliver and Hibbert [14], which, however, favored the old AEL designations. Percentage compositions of eigenvectors resulting from our calculations suggest that the configuration labels given in AEL for these two pairs of levels should be interchanged (see table 3). Nevertheless, to avoid confusion in line identifications we retained the AEL labels adopted also by Sansonetti and Martin [20].

Another type of excitation is represented by excitation of the inner $5s$ electron to the $5p$ shell, leading to the $5s5p^2$ configuration with seven levels containing a quartet and three doublet terms. For a long time it was difficult to observe the intercombination lines, as their transition probabilities are low. In the present work, we confirm six levels including $\ ^2P_{1/2}$ at 80455.8 cm^{-1} reported in AEL [4] as questionable. However, we could not confirm the $\ ^2S_{1/2}$ level reported at 80206.1 cm^{-1} . This level value was ambiguous for two reasons. Firstly, it strongly deviated from the LSF calculations. Secondly, its strongest predicted transition to the ground level was missing. Therefore, this level value was rejected. We further disagree with the recent verification of this level value by Alonso-Medina et al. [17] since all transitions involving this level are very weak, and those observed by Alonso-Medina et al. [17] together with the claimed uncertainties cannot be reconciled with other identified lines in this spectrum. Connerade and Baig [21] revised the identification of the $5s5p^2 \ ^2P_{1/2}$ and $\ ^2P_{3/2}$ levels by analyzing level separations along the In I

isoelectronic sequence. Their suggested values for these two levels were 80206 cm^{-1} and 81718 cm^{-1} , respectively. We confirmed and refined the second level. However, the first one, as noted above, was found to be spurious. Calculations of Connerade and Baig [21] yielded a predicted value for the $5s5p^2 \ ^2S_{1/2}$ level at 60024 cm^{-1} . We located this level at a much higher position, at 75954.4 cm^{-1} , by identifying transitions from it to both levels of the ground term. The strongest of these transitions (to $^2P_{1/2}$) was observed in our spectra at 1316.579 \AA . The transition to $^2P_{3/2}$, predicted to be much weaker, was not observed on our plates. However, it was observed by Wu [11] at 1394.667 \AA in two exposures. This newly revised level value fits well in our parametric LSF calculations with reasonable values of the fitted parameters. This identification is further validated by an isoelectronic comparison presented in figure 2 for the sequence In I to Xe VI. The $^2S_{1/2}$ and $^2P_{1/2}$ levels of $5s5p^2$ are strongly mixed in these spectra. In In I, the leading terms are 2S and 2P for the lower and upper of these two levels, respectively, while in Xe VI they are reversed. The currently adopted position of $5s5p^2 \ ^2S_{1/2}$ level in Sn II, indicated by dashed lines in figure 2, is strikingly inconsistent with the smooth isoelectronic trend of other data points. Our new LSF calculations for this sequence result in interchange of the term labels $^2S_{1/2}$ and $^2P_{1/2}$ in Te IV and predict a much lower position for the $^2S_{1/2}$ level in Sn II. This prediction is in qualitative agreement with findings of Connerade and Baig [21]. As indicated by the solid lines in figure 2, our revised identification produces a smooth isoelectronic trend for the lower $J=1/2$ level, similar to the behavior of the upper level. The revised level values and term labels, along with the calculated percentage compositions, are given in table 2. Additional support for our new identification of the $5s5p^2 \ ^2S_{1/2}$ level in Sn II is provided by a recent theoretical calculation by Oliver and Hibbert [14]. They predicted $^2S_{1/2}$ in Sn II to be at 76215 cm^{-1} , which is in close agreement with our newly found level value. Col3n and Alonso-Medina [22] suggested an explanation of the anomaly in the $5s5p^2 \ ^2S_{1/2}$ and $^2P_{1/2}$ levels of Sn II by the presence of some mysterious interacting configuration(s). As this anomaly is now resolved, their suggestion can be dismissed. It should be noted that these two levels are strongly mixed (see tables 2 and 3). Thus, their LS labels have little physical meaning and are used in our tables for bookkeeping purpose only.

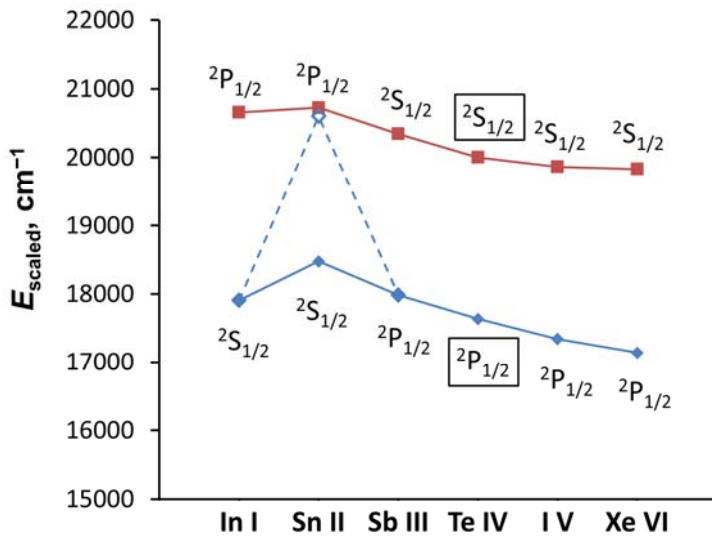


Figure 2 (color online). Isoelectronic comparison of scaled energies, $E_{\text{scaled}} = (E - 39000)/Z_c$, of the strongly mixed $5s5p^2 \ ^2S_{1/2}$ and $^2P_{1/2}$ levels. The dominant term labels of the lower and upper levels interchange at ionic core charge $Z_c = 3$ (Sb III). The open circle just below the $^2P_{1/2}$ data point for Sn II indicates the previously adopted position of the $^2S_{1/2}$ level in Sn II at 80206 cm^{-1} [4]. Dashed lines connecting this data point with the other ones of the lower level show how this graph would look if that incorrect value were used instead of our revised value (solid rhomb and solid lie). Solid boxes indicate the revised term labels for Te IV. See table 2 for details.

Table 2. The two $J = 1/2$ doublet levels of the $5s5p^2$ configuration in the In I isoelectronic sequence. All percentage compositions and the Sn II energies are from the present work; the rest of the data are from ASD [5].

Isoelectronic member	Lower level				Upper level			
	Energy, cm^{-1}	Percentages		Term label	Energy, cm^{-1}	Percentage		Term label
		^2S	^2P			^2S	^2P	
In I	56906	74	24	^2S	59657	23	76	^2P
Sn II	75954.4 ^a	51	46	^2S	80455.3	45	53	^2P
Sb III	92948.9	31	37	$^2\text{P}^b$	100030	57	41	^2S
Te IV	109536	40	57	$^2\text{P}^c$	119009	56	42	$^2\text{S}^c$
I V	125703	36	61	^2P	138328	60	38	^2S
Xe VI	141837	32	64	^2P	157995	62	36	^2S

^a Our revised value replaces the previously reported 80206 cm^{-1} [4].

^b Third leading component: 31 % of $5s^26s^2\text{S}$ (at 93422.5 cm^{-1}).

^c The level designations for Te IV are interchanged according to our LSF calculations.

4.2.2. The $5p^3$ and $5s5p(5d+6s)$ configurations

These configurations arise from excitation of the $5s5p^2$ configuration. In the sequence Sb III – I V [23–25], transitions from these configurations have been observed in the Antigonish laboratory with moderate intensity. Therefore, we expected them to occur in Sn II as well. Our preliminary calculations for Sn II show that these configurations strongly interact with each other and also with other configurations, e.g., $4f5s5d$ and $5p5d^2$, which are completely unknown at present. The $5p^3$ and $5s5p(5d+6s)$ configurations are predicted to extend past the ionization limit. Thus, many of their levels should be autoionizing, making the analysis more difficult. Additional complication stems from the fact that some of the levels of these configurations are embedded within highly excited levels of the $5s^2np$ and nf series, with which they strongly interact. A few levels of these configurations were listed in AEL [4] with incomplete designations; some were marked as doubtful. We attempted to improve interpretation of these levels. The level at 109223.4 cm^{-1} in AEL [4] is supported by two transitions terminating on the $5s5p^2 \ ^4\text{P}_{1/2,3/2}$ levels, observed in our spectra, and one transition to $5s^25d \ ^2\text{D}_{3/2}$ observed by Wu [11]. We now identified this level as $5s^210p \ ^2\text{P}_{1/2}$ on the basis of our LSF calculation. Observed relative intensities of the lines are in satisfactory agreement with calculations. We were able to confirm the quartet levels of $5s5p6s$ configuration listed in AEL [4], as they give rise to strong transitions to the lowest quartet levels of the $5s5p^2$ configuration. The level at 113819.0 cm^{-1} is also confirmed. In AEL [4], the J value of this level was given as $3/2$ with a question mark, and no configuration label was attributed to it. Our present calculation with extensive configuration interaction shows that this level should be assigned to $^2\text{D}_{3/2}$ of the $5s5p5d$ configuration.

As noted above, identification of autoionizing levels presented considerable difficulties. We could not confirm the level at 124627.7 cm^{-1} in AEL [4]. Wu [11] assigned three observed lines at 1520.153 \AA , 2907.33 \AA , and 7412.5 \AA to this level. However, no satisfactory match could be found for this level in our calculations. All other autoionizing levels given in AEL [4] have been identified in our spectra. In particular, three levels previously reported at 123156 , 132168 and 132708 cm^{-1} with uncertain designations are found to be associated with the $5p^3$ configuration. The first of them is identified as $5p^3 \ ^4\text{S}^{\circ}_{3/2}$, while the other two have dominant contributions of $5s5p(^1\text{P}^{\circ})5d \ ^2\text{D}^{\circ}_{3/2}$ and $^2\text{D}^{\circ}_{5/2}$, respectively. Since the $5s5p5d$ configuration strongly interacts with $5p^3$, these levels have large admixtures of $5p^3 \ ^2\text{D}^{\circ}$ in their wavefunctions. A few of the other autoionizing levels that were based on just one or two observed transitions remain questionable.

4.2.3. The $5s^2np$ and $5s^2nf$ configurations

After the successful establishment of the $5s^2ns$ and nd levels, a further analysis of the $5s^2np$ and nf configurations was undertaken. The $5s^2np$ ($n = 6-9$) and $5s^2nf$ ($n = 4-6$) configurations were already reported in AEL [4]. Some transitions from $5s^26p$ and $7p$ to levels of the $5s^26s$, $5s^25d$, and $5s5p^2$ configurations were measured interferometrically by Brill [10]. Lines arising from the $5s^2np$ ($n = 6-9$) configurations were classified by McCormick and Sawyer [6], and some additional lines were also observed by Wu [11]. We confirm all these identifications, as the observed level energies and relative line intensities are in satisfactory agreement with our calculations.

4.2.4. Levels of $5s^2ng$ configurations

The $5s^2ng$ ($n = 6-11$) 2G energy levels were established by transitions from the levels of $5s^24f$ configuration, identified primarily by McCormick and Sawyer [6]. Some of the transitions observed by McCormick and Sawyer were more accurately measured by Wu [11]. Brill [10] re-measured the 4f–6g transitions with much better accuracy. No discernible fine-structure splitting was detected in any of the observed $5s^2ng$ 2G multiplets. The lowest member of this series, $5s^25g$ 2G , was unknown so far. Brill [10] observed a pair of lines at 9058.880 Å and 9063.658 Å with a separation $5.818(6)$ cm^{-1} closely matching his measured $5s^24f$ $^2F^\circ$ $J = 5/2-7/2$ interval, $5.804(9)$ cm^{-1} . He recognized that these lines must correspond to transitions combining the $5s^24f$ $^2F^\circ_{5/2,7/2}$ levels with some unknown level, but he was unable to decide whether this level is located above or below $5s^24f$ $^2F^\circ$. Thus, he gave two possible energy values for this unknown level, $78258.194(6)$ cm^{-1} or $100324.103(6)$ cm^{-1} . By extrapolating the known energies of the $5s^2ng$ 2G terms with $n \geq 6$ to $n = 5$ with the core-polarization formula (see section 4.5), we found that the upper of these two suggested values almost exactly coincides with the predicted position of the $5s^25g$ 2G term. Our LSF calculations ruled out the existence of a level at the lower of the two positions suggested by Brill, that could possibly combine with $5s^24f$ $^2F^\circ$. Thus, we identified the level at $100324.103(6)$ cm^{-1} as $5s^25g$ 2G . Observed level energies and relative line intensities of all transitions from $5s^2ng$ levels agree well with our calculations.

4.3. Optimization of energy levels

To derive the energy level values that best fit all observed transition wavelengths, we used the least-squares level optimization program LOPT [26]. The crucial factors for the level optimization procedure are the correct identification of the spectral lines, estimation of their uncertainties, and absence of systematic shifts. Correctness of identifications was ensured by the analysis described above. Estimation of the statistical and systematic uncertainties of wavelengths was described in section 3. This estimation partially relies on the level optimization procedure, since some of the reference wavelengths used in this procedure are the Sn II Ritz wavelengths. Therefore, the level optimization was made in several iterations. In the initial stage, only the accurate measurements of Brill [10], as well as our measurements in the VUV, for which independent estimates of uncertainties are available, were included in the optimization. This resulted in initial estimates of the energy levels and Ritz wavelengths derived from them. Deviations of wavelengths observed by Wu [11] and by McCormick and Sawyer [6] from these Ritz wavelengths revealed systematic shifts smoothly varying with wavelength. After these systematic shifts were removed, residual deviations of corrected wavelengths from Ritz values provided a sufficient statistical basis to assign uncertainties to all the measurements. Then the corrected wavelengths from Wu [11] and McCormick and Sawyer [6] were also included in the level optimization, leading to an extended and more accurate set of energy levels and Ritz wavelengths. This process was repeated until the estimated systematic shifts stopped changing.

Table 3. Optimized energy levels of Sn II

Configuration	Term	J	Energy ^a cm^{-1}	Unc. ^b cm^{-1}	Leading percentages ^c	ΔE_{o-c} ^d	No. of lines ^e
$5s^25p$	$^2P^\circ$	1/2	0.00	0.04	97 2 $5p^3$	$^2P^\circ$ 81	17
$5s^25p$	$^2P^\circ$	3/2	4251.505	0.014	97 2 $5p^3$	$^2P^\circ$ -81	25
$5s5p^2$	4P	1/2	46464.301	0.018	98	-63	12
$5s5p^2$	4P	3/2	48368.198	0.007	99	-20	17
$5s5p^2$	4P	5/2	50730.237	0.005	97 3 $5s5p^2$	2D 80	12
$5s^26s$	2S	1/2	56886.3763	0.003	100	0	7
$5s5p^2$	2D	3/2	58844.194	0.004	41 58 $5s^25d$	2D -128	17
$5s5p^2$	2D	5/2	59463.494	0.005	38 59 $5s^25d$	2D 128	12
$5s^25d$	2D	3/2	71406.155	0.008	41 54 $5s5p^2$	2D -120	11
$5s^26p$	$^2P^\circ$	1/2	71493.287	0.003	99	3	14
$5s^25d$	2D	5/2	72048.273	0.007	40 56 $5s5p^2$	2D 119	12
$5s^26p$	$^2P^\circ$	3/2	72377.4616		99	-3	16
$5s5p^2$	2S	1/2	75954.4	R 0.3	51 46 $5s5p^2$	2P 105	3
$5s5p^2$	2P	1/2	80455.3	C 0.3	53 45 $5s5p^2$	2S -120	3
$5s5p^2$	2P	3/2	81718.43	0.24	97 2 $5s5p^2$	2D 18	3
$5s^27s$	2S	1/2	86280.332	0.005	99	0	5
$5s^24f$	$^2F^\circ$	7/2	89288.268	0.007	96 3 $4f5p^2$	$^2F^\circ$ -1	10
$5s^24f$	$^2F^\circ$	5/2	89294.068	0.006	96 3 $4f5p^2$	$^2F^\circ$ 1	11

Configuration	Term	J	Energy ^a cm ⁻¹	Unc. ^b cm ⁻¹	Leading percentages ^c			ΔE_{o-c} ^d	No. of lines ^e	
5s ² 6d	² D	3/2	90241.568	0.004	97	2	5s5p ²	² D	-27	7
5s ² 6d	² D	5/2	90351.908	0.005	97	2	5s5p ²	² D	26	6
5s ² 7p	² P ^o	1/2	91903.958	0.015	99				-2	6
5s ² 7p	² P ^o	3/2	92268.119	0.009	99				2	10
5s ² 8s	² S	1/2	98402.425	0.006	100				0	5
5s ² 5f	² F ^o	7/2	99660.991	0.006	99				-1	4
5s ² 5f	² F ^o	5/2	99666.340	0.006	99				1	4
5s ² 7d	² D	3/2	100284.125	0.010	99				-11	6
5s ² 5g	² G	7/2	100324.124	C 0.007	100				0	2
5s ² 5g	² G	9/2	100324.124	C 0.007	100				0	1
5s ² 7d	² D	5/2	100338.960	0.009	99				11	2
5s ² 8p	² P ^o	1/2	101204.2	0.4	99				4	2
5s ² 8p	² P ^o	3/2	101387.18	0.21	99				1	5
5s ² 9s	² S	1/2	104678.43	0.10	100				0	6
5s ² 6f	² F ^o	7/2	105360.3	1.8	99				9	1
5s ² 6f	² F ^o	5/2	105371.7	N 0.3	99				17	2
5s ² 8d	² D	3/2	105731.2	0.3	100				-6	5
5s ² 6g	² G	7/2	105737.495	0.007	100				0	2
5s ² 6g	² G	9/2	105737.495	0.007	100				0	1
5s ² 8d	² D	5/2	105763.02	0.23	100				6	3
5s ² 9p	² P ^o	1/2	106256.4	N 0.3	99				-28	2
5s ² 9p	² P ^o	3/2	106370.2	0.4	99				-26	3
5s ² 10s	² S	1/2	108357.6	0.4	100				0	4
5s ² 7g	² G	7/2	109002.3	0.4	100				0	2
5s ² 7g	² G	9/2	109002.3	0.4	100				0	1
5s ² 9d	² D	3/2	109006.2	0.4	100				-4	3
5s ² 9d	² D	5/2	109025.68	0.15	100				4	4
5s ² 10p	² P ^o	1/2	109222.18	R 0.23	81	16	5s5p(³ P ^o)6s	⁴ P ^o	61	3
5s5p(³ P ^o)6s	⁴ P ^o	1/2	109454.05	0.18	81	18	5s ² 10p	² P ^o	-13	2
5s ² 11s	² S	1/2	110699	4	100				1	1
5s5p(³ P ^o)6s	⁴ P ^o	3/2	110777.85	0.12	79	12	5s ² 11p	² P ^o	-11	5
5s ² 8g	² G	7/2	111120.8	0.4	100				0	2
5s ² 8g	² G	9/2	111120.8	0.4	100				0	1
5s ² 10d	² D	3/2	111122.6	1.2	100				-7	2
5s ² 10d	² D	5/2	111143.3	1.1	100				5	4
5s ² 9g	² G	7/2	112574.0	0.8	100				0	2
5s ² 9g	² G	9/2	112574.0	0.8	100				0	1
5s ² 11d	² D	3/2	112574.1	N 0.5	100				-8	2
5s ² 11d	² D	5/2	112596.9	1.1	100				9	3
5s ² 10g	² G	7/2	113610.5	1.5	100				0	2
5s ² 10g	² G	9/2	113610.5	1.5	100				0	1
5s5p(³ P ^o)5d	² D ^o	5/2	113818.68	R 0.18	62	18	5p ³	² D ^o	44	4
5s5p(³ P ^o)6s	² P ^o	1/2	113952.66	N 0.13	30	50	5s ² 14p	² P ^o	9	6
5s5p(³ P ^o)6s	⁴ P ^o	5/2	114245.98	0.14	95	2	5s5p(³ P ^o)5d	² D ^o	9	6
5s ² 11g	² G	7/2,9/2	114378.1	2.2	100				0	1
5s ² 11g	² G	7/2,9/2	114378.1	2.2	100				0	1
5s5p(³ P ^o)5d	⁴ F ^o	5/2	115256.35	N? 0.22	76	8	5s5p(³ P ^o)5d	² D ^o	-31	1
5s5p(³ P ^o)5d	⁴ F ^o	7/2	116423.4	N 0.3	50	41	5s ² 19f	² F ^o	-49	3
Sn III 5s ² ¹ S ₀	Limit		118023.7	R 0.5						
5s5p(³ P ^o)5d	⁴ D ^o	1/2	119981.3	R? 0.4	93	4	5s5p(³ P ^o)5d	⁴ P ^o	-116	2
5s5p(³ P ^o)5d	⁴ D ^o	3/2	120064.5	R? 0.4	76	16	5s5p(³ P ^o)5d	⁴ P ^o	-73	2
5s5p(³ P ^o)5d	⁴ D ^o	5/2	120253.85	R 0.23	52	39	5s5p(³ P ^o)5d	⁴ P ^o	54	3
5s5p(³ P ^o)5d	⁴ D ^o	7/2	122491.6	R? 0.5	92	7	5s5p(³ P ^o)5d	⁴ F ^o	102	1
5p ³	⁴ S ^o	3/2	123156.8	R 0.3	88	5	5p ³	² P ^o	-2	4
5s5p(³ P ^o)5d	⁴ P ^o	5/2	123688.3	N 0.4	55	41	5s5p(³ P ^o)5d	⁴ D ^o	60	2
5s5p(³ P ^o)5d	⁴ P ^o	3/2	124245.80	R 0.16	80	18	5s5p(³ P ^o)5d	⁴ D ^o	15	8
5s5p(³ P ^o)5d	⁴ P ^o	1/2	124524.4	N? 0.6	94	5	5s5p(³ P ^o)5d	⁴ D ^o	-13	1

Configuration	Term	J	Energy ^a cm ⁻¹	Unc. ^b cm ⁻¹	Leading percentages ^c	ΔE_{o-c} ^d	No. of lines ^e
5s5p(¹ P ^o)5d	² D ^o	3/2	132168.95	R 0.17	51 32 5p ³	² D ^o -382	4
5s5p(¹ P ^o)5d	² D ^o	5/2	132708.1	R 0.3	54 32 5p ³	² D ^o 365	4

^aSymbols next to the energy value have the following meaning: C – previous tentative identification has been confirmed here; N – new identification; R – previous value and/or interpretation has been revised here; ? – questionable identification.

^bUncertainties resulting from the level optimization procedure are given on the level of one standard deviation. They correspond to uncertainties of level separations from 5s²6p ²P^o_{3/2}. To determine uncertainties of excitation energies from the ground level, the given values should be combined in quadrature with the uncertainty of the ground level, 0.04 cm⁻¹.

^cThe first percentage value refers to the configuration and term given in the first two columns of the table. The second percentage value refers to the configuration and term given next to it. The percentage compositions were determined in this work by a parametric least-squares fitting with Cowan's codes [19] (see text).

^dDifferences between observed energies and those calculated in the parametric least squares fitting.

^eNumber of observed lines determining the level in the optimization procedure.

The final list of optimized energy levels is given in table 3. In this table, the level uncertainties are given for separations from the 5s²6p ²P^o_{3/2} level. This level was chosen as the base, because it has the largest number of accurately measured transitions. To infer the uncertainty of an excitation energy from the ground level, one should combine the given uncertainty value in quadrature with the uncertainty of the ground level, 0.04 cm⁻¹. It can be seen that the level uncertainties vary greatly, from 0.003 cm⁻¹ to 4 cm⁻¹, depending on the number and measurement accuracy of the lines determining the level. With a few exceptions, the level values are rounded using the “rule of 24,” i.e., the uncertainty of the value does not exceed 24 units of the least significant digit of the value. In a few cases, an additional significant figure was required in order to reproduce the precisely measured transition wavelengths.

Some of the results of our LSF calculations, such as percentage compositions and differences of observed energies from those calculated in the parametric fitting are also given in table 3. The fitted parameter values obtained in the LSF are given in table 4.

Table 4. LSF parameters (cm⁻¹) for Sn II

Configuration	Parameter	LSF	Group ^a	STD	HFR	LSF/HFR
Odd Parity^b						
5s ² 5p	E_{av}	6860.3		116	0.0	
	$\zeta(5p)$	3016.3	1	83	2665.8	1.1315
5s ² 6p	E_{av}	72666.4		111	70522.8	1.0304
	$\zeta(6p)$	610.5	1	17	539.6	1.1314
5s ² 7p	E_{av}	92361.0		111	90536.8	1.0201
	$\zeta(7p)$	246.7	1	7	218.0	1.132
5s ² 8p	E_{av}	101458.0		111	99608.5	1.0186
	$\zeta(8p)$	127.0	1	3	112.2	1.132
5s ² 9p	E_{av}	106459.7	4	99	104563.0	1.0181
	$\zeta(9p)$	74.2	1	2	65.6	1.132
5s ² 10p	E_{av}	109339.8	4	101	107572.2	1.0164
	$\zeta(10p)$	47.2	1	1	41.7	1.132
5s ² 11p	E_{av}	111223.6	4	103	109540.5	1.0154
	$\zeta(11p)$	31.8	1	1	28.1	1.132
5s ² 12p	E_{av}	112521.2	4	104	110896.3	1.0147
	$\zeta(12p)$	22.5	1	1	19.9	1.131
5s ² 13p	E_{av}	113454.3	4	105	111871.2	1.0142

Configuration	Parameter	LSF	Group ^a	STD	HFR	LSF/HFR
	$\zeta(13p)$	16.4	1	0	14.5	1.131
5s ² 14p	E_{av}	114151.8	4	106	112600.0	1.0138
	$\zeta(14p)$	12.4	1	0	11.0	1.13
5s ² 15p	E_{av}	114680.1	4	106	113152.0	1.0135
	$\zeta(15p)$	9.6	1	0	8.5	1.13
5s ² 16p	E_{av}	115095.4	4	107	113585.9	1.0133
	$\zeta(16p)$	7.6	1	0	6.7	1.13
5s ² 17p	E_{av}	115427.6	4	107	113933.0	1.0131
	$\zeta(17p)$	6.0	1	0	5.3	1.13
5s ² 18p	E_{av}	115694.7	4	107	114212.1	1.0130
	$\zeta(18p)$	4.9	1	0	4.3	1.14
5s ² 19p	E_{av}	115910.3	4	108	114437.3	1.0129
	$\zeta(19p)$	4.1	1	0	3.6	1.14
5s ² 20p	E_{av}	116095.8	4	108	114631.2	1.0128
	$\zeta(20p)$	3.4	1	0	3.0	1.13
4f5s ²	E_{av}	93783.8		114	87380.8	1.0733
	$\zeta(4f)$	0.4		fixed	0.4	1.0000
5s ² 5f	E_{av}	99981.2		112	97859.7	1.0217
	$\zeta(5f)$	0.2		fixed	0.2	1.0000
5s ² 6f	E_{av}	105538.7	5	107	103503.1	1.0197
	$\zeta(6f)$	0.1		fixed	0.1	1.0000
5s ² 7f	E_{av}	108779.9	5	110	106886.6	1.0177
	$\zeta(7f)$	0.1		fixed	0.1	1.0000
5s ² 8f	E_{av}	110873.6	5	112	109072.3	1.0165
	$\zeta(8f)$	0.1		fixed	0.1	1.0000
5s ² 9f	E_{av}	112303.7	5	114	110565.2	1.0157
5s ² 10f	E_{av}	113325.1	5	115	111631.4	1.0152
5s ² 11f	E_{av}	114076.2	5	116	112415.5	1.0148
5s ² 12f	E_{av}	114646.3	5	116	113010.6	1.0145
5s ² 13f	E_{av}	115090.9	5	117	113474.8	1.0142
5s ² 14f	E_{av}	115440.1	5	117	113839.3	1.0141
5s ² 15f	E_{av}	115719.7	5	117	114131.2	1.0139
5s ² 16f	E_{av}	115953.9	5	118	114375.6	1.0138
5s ² 17f	E_{av}	116144.1	5	118	114574.2	1.0137
5s ² 18f	E_{av}	116301.7	5	118	114738.7	1.0136
5s ² 19f	E_{av}	116444.8	5	118	114888.1	1.0135
5s ² 20f	E_{av}	116564.1	5	118	115012.6	1.0135
5s5p6s	E_{av}	118905.2		211	109900.0	1.0819
	$\zeta(5p)$	3492.9	1	96	3087.0	1.1315
	$G^1(5s5p)$	29907.8	6	454	51164.2	0.5845
	$G^0(5s6s)$	1745.8	9	246	2522.8	0.6920
	$G^1(5p6s)$	2925.9	9	413	4228.1	0.6920
5s5p5d	E_{av}	128129.4		152	117237.6	1.0929
	$\zeta(5p)$	3415.7	1	94	3018.8	1.1315

Configuration	Parameter	LSF	Group ^a	STD	HFR	LSF/HFR
5p ³	$\zeta(5d)$	77.2		fixed	77.2	1.0000
	$F^2(5p5d)$	20634.2		865	20388.4	1.0121
	$G^1(5s5p)$	29712.1	6	451	50829.4	0.5845
	$G^2(5s5d)$	10985.9		1189	9761.6	1.1254
	$G^1(5p5d)$	18655.8	7	663	20189.5	0.9240
	$G^3(5p5d)$	11538.5	7	410	12487.0	0.9240
	E_{av}	136589.5		179	127058.9	1.0750
	$F^2(5p5p)$	32281.3		fixed	37046.5	0.8714
	$\zeta(5p)$	3064.7	1	84	2708.6	1.1315
	E_{av}	262609.7		fixed	255939.8	1.0261 ^c
5p5d ^{2c}	$\zeta(5p)$	3732.4	1	103	3298.7	1.1315
4f5p ^{2c}	E_{av}	220238.9		fixed	213569.0	1.0312 ^c
4f5s5d ^c	$\zeta(5p)$	3621.3	1	100	3200.5	1.1315
	E_{av}	223939.3		fixed	217269.4	1.0307 ^c
Even Parity						
5s5p ²	E_{av}	63956.0		36	55474.7	1.1529
	$F^2(5p5p)$	32090.9		286	36826.8	0.8714
	$\zeta(5p)$	3040.9		57	2681.9	1.1339
	$G^1(5s5p)$	30953.3		109	48632.5	0.6365
5s ² 6s	E_{av}	56981.0		77	55518.4	1.0263
5s ² 7s	E_{av}	86243.4		77	84679.3	1.0185
5s ² 8s	E_{av}	98398.8		77	96666.1	1.0179
5s ² 9s	E_{av}	104677.5		77	102872.0	1.0176
5s ² 10s	E_{av}	108357.2		77	106511.0	1.0173
5s ² 11s	E_{av}	110698.2	2	77	108830.1	1.0172
5s ² 12s	E_{av}	112202.1	2	78	110399.3	1.0163
5s ² 5d	E_{av}	64921.4		100	64114.7	1.0126
	$\zeta(5d)$	66.7		fixed	66.7	1.0000
	E_{av}	89806.5		56	88201.0	1.0182
5s ² 6d	$\zeta(6d)$	26.7		fixed	26.7	1.0000
	E_{av}	100165.1		55	98423.5	1.0177
5s ² 7d	$\zeta(7d)$	13.7		fixed	13.7	1.0000
	E_{av}	105680.4		54	103874.8	1.0174
5s ² 8d	$\zeta(8d)$	7.9		fixed	7.9	1.0000
	E_{av}	108979.1		54	107136.5	1.0172
5s ² 9d	$\zeta(9d)$	5.0		fixed	5.0	1.0000
	E_{av}	111111.2		54	109247.0	1.0171
5s ² 10d	$\zeta(10d)$	3.3		fixed	3.3	1.0000
	E_{av}	112569.7	3	54	110689.9	1.0170
5s ² 11d	$\zeta(11d)$	2.3		fixed	2.3	1.0000
	E_{av}	113560.6	3	55	111722.9	1.0164
5s ² 12d	$\zeta(12d)$	1.7		fixed	1.7	1.0000
	E_{av}	100389.8		54	98428.2	1.0199

Configuration	Parameter	LSF	Group ^a	STD	HFR	LSF/HFR
5s ² 6g	$\zeta(5g)$	0.1		fixed	0.1	1.0000
	E_{av}	105776.4		54	103823.2	1.0188
5s ² 7g	$\zeta(6g)$	0.1		fixed	0.1	1.0000
	E_{av}	109026.5		54	107087.6	1.0181
5s ² 8g	$\zeta(7g)$	0.0		fixed	0.0	
	E_{av}	111136.7		54	109207.1	1.0177
5s ² 9g	$\zeta(8g)$	0.0		fixed	0.0	
	E_{av}	112585.0		54	110660.2	1.0174
5s ² 10g	$\zeta(9g)$	0.0		fixed	0.0	
	E_{av}	113618.4		54	111699.7	1.0172
5s ² 11g	$\zeta(10g)$	0.0		fixed	0.0	
	E_{av}	114383.9	4	54	112466.0	1.0171
5s ² 12g	$\zeta(11g)$	0.0		fixed	0.0	
	E_{av}	114944.3	4	55	113049.7	1.0168
4f5s5p ^c	E_{av}	148823.6		fixed	142153.7	1.0469 ^c
5s5d ^{2c}	E_{av}	196200.2		fixed	189530.3	1.0352 ^c
Configuration interaction ^d						
5s5p ² -5s ² 5d	$R^1(5p5p,5s5d)$	18161.1	1	124	27501.0	0.6604
5s5p ² -5s ² 6d	$R^1(5p5p,5s6d)$	9433.0	1	64	14284.3	0.6604
5s5p ² -5s ² 7d	$R^1(5p5p,5s7d)$	6265.9	1	43	9488.4	0.6604
5s5p ² -5s ² 8d	$R^1(5p,5p,5s,8d)$	4595.3	1	31	6958.6	0.6604
5s5p ² -5s ² 9d	$R^1(5p5p,5s9d)$	3570.9	1	24	5407.4	0.6604
5s5p ² -5s ² 10d	$R^1(5p5p,5s10d)$	2884.5	1	20	4368.0	0.6604
5s5p ² -5s ² 11d	$R^1(5p5p,5s11d)$	2396.1	1	16	3628.4	0.6604
5s5p ² -5s ² 12d	$R^1(5p5p,5s12d)$	2033.2	1	14	3078.9	0.6604

^a Parameters in each numbered group were linked together with their ratio fixed at the Hartree-Fock level.

^b All configuration-interaction parameters R^k for the odd configurations were fixed at 80 % of the Hartree-Fock value.

^c These highly excited configurations are unknown experimentally. They were included in the calculations in order to account for their interaction with other configurations studied in this work. Except for the average energies E_{av} given here and $\zeta(5p)$ for 5p5d² and 4f5p², all other parameters of these configurations were fixed at the 80 % of the Hartree-Fock values (F^k , G^k , R^k) or 100 % of the Hartree-Fock values (ζ).

^d Other R^k parameters of the even configurations were fixed at 80 % of the Hartree-Fock value.

Natural tin consists of ten stable isotopes with abundances ranging from 0.3 % to 33 %. Three of these isotopes have nuclear spin 1/2 and a rather large nuclear magnetic moment about $-1.0 \mu_N$. Thus, lines observed from samples of natural tin (which were used in all experimental works quoted in the present paper) must be broadened by isotope shifts and hyperfine structure. Since there is no such entity as an atom of natural tin, the energy levels derived by our level optimization do not correspond to any physical object but are empirical values that best describe the observed spectral lines. This should be kept in mind when using the high-precision values from tables 1 and 3. Asymmetry of line profiles caused by isotope shifts and hyperfine structure may result in deviations of observed peak wavelengths from the Ritz values given in table 1. Observed isotope shifts between adjacent even isotopes are typically $(0.005-0.02) \text{ cm}^{-1}$, while the hyperfine structure in less abundant odd isotopes is an order of magnitude larger. References to studies of isotope shifts and hyperfine structure of Sn II can be obtained from the NIST Atomic Energy Levels and Spectra Bibliographic Database at <http://physics.nist.gov/Elevbib>.

For completeness, we note that there is only one reported measurement of the Landé g -factor for Sn II. Namely, David et al. [27] accurately measured the Landé g -factor for the $5s5p^2\ ^4P_{3/2}$ level to be 2.6609(7).

4.4. Intensities of observed lines

In the history of atomic spectroscopy, it has been an unfortunate long-standing tradition to give very rough estimates of relative intensities of observed lines. Although line intensities were always recognized to be important in correct identification of transitions causing them, the arguments had to be qualitative because the sensitivity of registration strongly varies with wavelength and depends on rarely quantified properties of detectors, spectrographs, and optics used. Also, different excitation conditions in light sources lead to large variations in line intensities. A method suggested and successfully used in a recent series of papers [28–30] overcomes these problems and allows one to reduce line intensities observed by different authors using different equipment to a common uniform scale. The method is based on using the Boltzmann equation to approximate populations of energy levels together with theoretically estimated radiative rates. It was shown in the papers quoted above that this approximation in most cases allows one to describe the observed intensities by a simple formula with weighted transition rate (gA) multiplied by a Boltzmann factor with a suitable effective excitation temperature. Then spectral response functions of the registration equipment can easily be derived by comparing observed and modeled intensities, and intensities observed with different setups can be reduced to a uniform scale with a common excitation temperature. Deviations of plasma conditions from the local thermodynamic equilibrium (LTE) and inaccuracies in estimated transition rates and derived response functions of registration equipment typically lead to errors of about a factor of three in such modeled intensities. Nevertheless, thus derived intensities provide a robust quantitative criterion for line identification and can even be used to estimate transition rates, when such estimates cannot be obtained from theory. Of course, the above-mentioned factor-of-three uncertainty is a restriction for many applications, but there are many cases where such estimates can be useful.

This method was applied to obtain the reduced relative intensities given in table 1. Below, we explain reduction of intensities for each set of observations.

The Boltzmann plot for our observed line intensities, shown in figure 3a, indicates an effective excitation temperature of 2.0 eV in our triggered spark source. This plot was built with intensities corrected for the variation of response function of our equipment with wavelength, denoted as I_{corr} . The logarithmic intensity-correction function $F(\lambda)$ used for this correction is shown in figure 3b. Correction is made by multiplying the observed intensities by exponent of $F(\lambda)$. Transition rates gA used in the Boltzmann plots were calculated with Cowan's codes using our fitted parameters from the LSF.

Similarly, figures 3c and 3d present the Boltzmann plot and intensity-correction function for exposure 1 in Wu's line list [11]. It should be noted that the quantity given by Wu in the intensity columns is actually transparency (not the commonly used darkening) of the photographic plate on the scale 0 to 1000. To obtain the intensities, we subtracted his transparency values from 1000. Effective temperature in the source used for exposure 1 turned out to be 4.2 eV, which is the highest for all light sources used in the published literature. Apparently, this high temperature allowed Wu to observe lines from very highly excited levels not observed in other experiments. Reduction of intensities observed in the other three exposures reported by Wu [11] was made in a similar way. Effective temperatures for his exposures 2, 3, and 4 turned out to be about 3.6 eV, 3.7 eV, and 3.8 eV, respectively. Response functions derived from exposures 2 and 3, which cover the same wavelength range as exposure 1, are similar to the one shown in figure 3d. For the final reduction of Wu's intensity values, we used the correction function averaged over these three exposures.

It should be noted that, despite the non-linear properties of photographic plates, the original observed intensities in both our and Wu's work did not show any significant non-linearity with exposure. This can easily be verified by plotting the ratio of calculated and observed intensities versus the observed intensity. Non-linearity would result in a trend on such plots, which was not detected.

Intensities observed by Brill [10] and by McCormick and Sawyer [6] were reduced by the same method as described above. The effective excitation temperature in the light source used by Brill was found to be 1.9 eV, which is close to our triggered-spark value of 2.0 eV.

For the light source used by McCormick and Sawyer [6], the effective temperature was found to be somewhat lower, about 1.4 eV.

After the variations of response functions of registration equipment were removed from the observed intensities, and the effective temperatures were determined for each set of observations, it was easy to scale the corrected observed intensities to the same effective temperature. We chose the highest temperature in all sets of measurements, 4.2 eV, as the basis for the unified scale. This choice is motivated by the need to have the smallest range of final intensity values, which is convenient for presentation purposes.

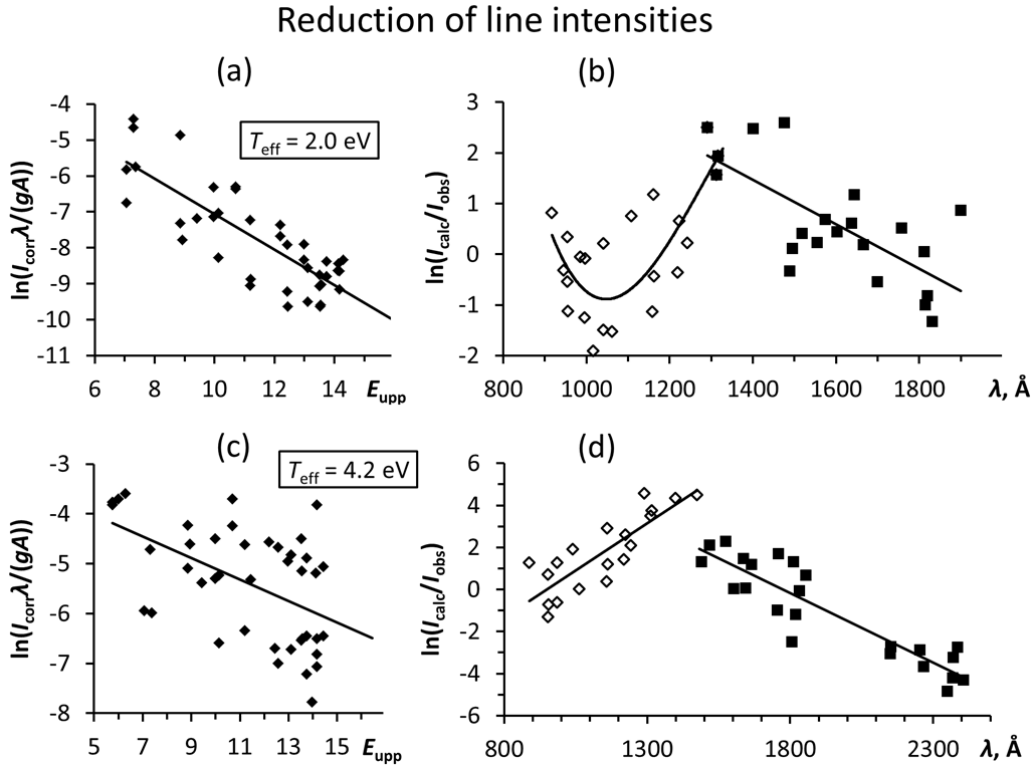


Figure 3. Boltzmann plots (a, c) and logarithmic intensity-correction functions (b, d) for our observations and those of Wu [11]. The upper-level energies E_{upp} in the Boltzmann plots are given in eV. The effective temperatures derived from the negative slope of the Boltzmann plots are shown in boxes. The calculated intensities I_{calc} in panels b and d are obtained from weighted transition rates gA calculated in the present work with a formula $I_{\text{calc}} = (gA/\lambda)\exp(-E_{\text{upp}}/T_{\text{eff}})$.

4.5. Ionization potential

The ionization potential (IP) given in AEL [4] is the value obtained by McCormick and Sawyer [6] using the $5s^2ng$ ($n = 6-11$) series. As the $5g$ level was established in the present work, and the measurements of McCormick and Sawyer contained significant systematic shifts, the IP has to be revised. We obtained the new value of IP using both the Ritz-type quantum-defect series extrapolation and core-polarization formula fitting for the $5s^2ng \ ^2G$ ($n = 5-11$) series using computer codes RITZPL and POLAR [31]; both leading to almost the same value. The formulas used in these series-fitting computer codes and explanation of their application can be found, for example, in reference [28]. The IP obtained from RITZPL using the two-parameter extended Ritz formula was $118023.6(7) \text{ cm}^{-1}$ and that from POLAR was $118023.8(7) \text{ cm}^{-1}$. Fitting of the three-parameter extended Ritz formula for the $5s^2ns$ ($n = 6-11$) series yields $118036.4(2) \text{ cm}^{-1}$ for the ionization energy. It is known that the ns series is slightly perturbed by an interaction with $5s5p^2 \ ^2S_{1/2}$. The ng series is free from such perturbations. Therefore, we adopted the average IP value obtained from the two fits of the $5s^2ng$ series, $118023.7(5) \text{ cm}^{-1}$, which is equivalent to

14.63307(6) eV. All fits were made using weights inversely proportional to squared uncertainties of the level values from table 2 combined in quadrature with the uncertainty of the ground level, 0.04 cm^{-1} . Our value is 6.7 cm^{-1} higher than the previously recommended value from McCormick and Sawyer [6].

5. Comparison with observed Auger electron spectrum

The Auger electron spectrum of Sn I and Sn II in the low-energy region 0–20 eV was observed by Forrest et al. [32] in a crossed atomic and electron beams experiment. They assigned several observed peaks to autoionization decay of the $4d^9 5s^2 5p^2$ configuration of Sn II, not considered in this work. In addition, they tentatively assigned a strong peak observed at 2.529 eV to the autoionization decay of the $5p^3 \ ^2P^\circ$ term of Sn II. This assignment does not agree with our identifications. According to our parametric fitting, the $5p^3$ configuration is highly mixed with $5s5p5d$, and the largest contribution of $5p^3 \ ^2P^\circ$ is predicted for the levels with large contributions from $5s5p(^3P^\circ)5d \ ^2P^\circ$ at about 128000 cm^{-1} and $5s5p(^1P^\circ)5d \ ^2P^\circ$ at about 152000 cm^{-1} . Autoionization decay of these levels to the $5s^2$ ground state of Sn III would produce Auger peaks at about 1.2 eV and 4.3 eV, respectively. Forrest et al. [32] observed a weak peak at 1.023 eV and medium-strength peaks at 4.117 eV and 4.277 eV, which may be associated with these predicted levels. However, for the peak at 1.023 eV our calculations yield a higher autoionization rate from a close predicted $5s5p(^3P^\circ)5d \ ^2F^\circ_{5/2}$ level at about 127000 cm^{-1} .

A few of the peaks observed by Forrest et al. [32] closely match the experimental energies of autoionizing Sn II levels we derived from our observed optical spectrum. In particular, the peaks observed at 1.761 eV and 1.829 eV closely match the predicted Auger energies for the $5s5p(^1P^\circ)5d \ ^2D^\circ$ $J=3/2$ and $5/2$ levels (observed at $132168.95 \text{ cm}^{-1}$ and 132708.1 cm^{-1}), respectively.

The peak observed at 0.657 eV can be a blend of Auger decays of the $5p^3 \ ^4S^\circ_{3/2}$ and $5s5p(^3P^\circ)5d \ ^4P^\circ_{5/2}$ levels (which we observed at 123156.8 cm^{-1} and 123688.3 cm^{-1} , respectively). These decays are predicted to be of comparable strengths, due to small admixtures of doublet terms in the composition of these levels.

The peak at 0.285 eV was assigned by Forrest et al. [32] to the decay of the Sn I $5s5p^3 \ ^3P^\circ_1$ and level to the $5s^2 5p \ ^2P^\circ_{1/2}$ ground level of Sn II. However, this assignment was later rejected by Dembczynski and Wilson [33]. This peak closely matches our observed energy for the Sn II $5s5p(^3P^\circ)5d \ ^4D^\circ_{5/2}$ level ($120253.85 \text{ cm}^{-1}$, corresponding to the Auger electron energy of 0.2773 eV), while the observed peak at 0.523 eV matches the decay of the $5s5p(^3P^\circ)5d \ ^4D^\circ_{7/2}$ level (122491.6 cm^{-1} , corresponding to the Auger electron energy of 0.5548 eV).

Finally, our calculations predict the metastable $5s5p(^3P^\circ)5d \ ^4F^\circ_{9/2}$ level at 118700 cm^{-1} . Autoionization of this level should produce an Auger peak at ejected electron energy of 0.088 eV. The strongest peak observed by Forrest et al. [32] is at 0.053 eV. This peak may be due to the decay of this metastable level.

We note that autoionization rates calculated for the Sn II levels discussed in this section are unreliable, because they strongly depend on very small mixing between doublet and quartet levels and on poorly known interaction between the $5p^3$ and $5s5p5d$ configurations. This, as well as the low resolution of the observed Auger electron spectrum [32], precludes definite identification of the observed Auger features. More sophisticated calculations, as well as higher-resolution experiments, are needed to elucidate the structure of autoionizing Sn II levels in the region just above the first ionization limit.

6. Transition probabilities

Oliver and Hibbert [14] made a large-scale Breit-Pauli configuration-interaction (CI) calculation of transition probabilities of Sn II using the CIV3 code of Hibbert and co-workers (see references in [14]). They presented three sets of results: one for their *ab initio* calculation (in the length gauge) and two for the fine-tuned calculation (one in the length gauge and the other in the velocity gauge). The fine tuning consisted of semiempirical adjustment of the diagonal matrix elements of the Hamiltonian minimizing the differences between the calculated and experimental eigenvalues. The line strengths S_L obtained in the length gauge in the fine-tuned calculation are considered to be the most accurate ones from the three sets. Their accuracy can be assessed by comparing them with the other two data sets, S_v (fine-tuned, velocity gauge) and S_{ab} (*ab initio*, length gauge). This comparison, illustrated in figure 4, shows that for strong lines with $S_L > 0.28$ the length and velocity forms of line strength agree within 6 % on average, while for

weaker lines with $S_L = (0.03-0.28)$ the agreement is somewhat worse, about 12 % on average. We adopted these standard deviations as conservative estimates of uncertainties of S_L in the corresponding ranges of line strength.

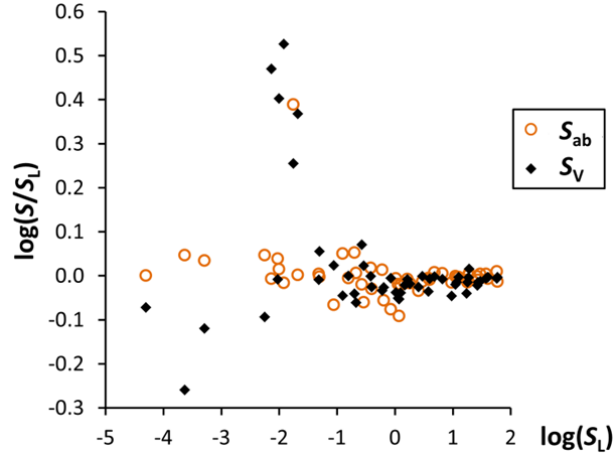


Figure 4. (Color online) Comparison of line strengths S calculated by Oliver and Hibbert [14] in different approximations and gauges: S_L – fine-tuned calculation in length gauge; S_V – fine-tuned calculation in velocity gauge; S_{ab} – *ab initio* calculation in length gauge.

For the ten weakest lines with $S_L < 0.03$, the length and velocity forms strongly disagree with each other. Most of these transitions are intercombination ones between doublet and quartet levels. As pointed out by Oliver and Hibbert [14], for such transitions, calculation of the line strength in velocity gauge requires additional terms not accounted for in the CIV3 code. This makes the comparison meaningless for intercombination transitions. Instead, the comparison of the *ab initio* and fine-tuned calculations in the length gauge can be used for estimating their uncertainties. Except for one large deviation for the $5s^25p^2P^{\circ}_{3/2} - 5s5p^2S_{1/2}$ transition at 1394.667 Å, S_{ab} agrees with S_L within 12 %. However, because of low statistics, we adopt a conservative estimate of 35 % for the uncertainty of transitions with $S_L = (0.001-0.03)$ and omit the three weakest transitions, for which the transition rate given by Oliver and Hibbert [14] strongly contradicts the observed line intensities.

The high accuracy of calculations of Oliver and Hibbert [14] for strong lines is further confirmed by comparison of calculated and observed radiative lifetimes presented in table 5.

David et al. [27], employing the direct magnetic resonance method, measured the lifetime of the $5s5p^24P_{1/2}$ level in Sn II to be 325(40) ns. They supported this result by two additional less accurate measurements with two independent methods.

Schectman et al. [15] measured the lifetimes of three levels, $5s^25d^2D_{3/2,5/2}$ and $5s^24f^2F^{\circ}_{5/2}$, with a beam-foil method. Using a similar method, Andersen and Lindgård [16] measured the lifetime of the $5s^26s^2S_{1/2}$ and $5s^25d^2D_{3/2}$ levels. Both these studies carefully accounted effects of cascades on the measured decay curves.

Table 5. Comparison of observed and calculated lifetimes in Sn II

Level		Energy cm ⁻¹	τ_{obs} ns	Ref. ^a	τ_{th} ns	Ref. ^a
5s5p ²	⁴ P _{1/2}	46464.301	325(40) 1500 ^b	D80 AM00	375 215 237	OH10 TW AM05
5s ² 6s	² S _{1/2}	56886.3763	1.10(10)	AL77	1.16 1.20 1.13	OH10 TW AM05
5s ² 5d	² D _{3/2}	71406.155	0.44(2) 0.50(5)	S00 AL77	0.45 0.37 0.41	OH10 TW AM05
5s ² 5d	² D _{5/2}	72048.273	0.46(4)	S00	0.51 0.45 0.50	OH10 TW AM05
5s ² 4f	² F ^o _{7/2}	89288.268	5.0(10)^c 6.9 ^b	GV85 AM00	3.82 3.28 3.21	OH10 TW AM05
5s ² 4f	² F ^o _{5/2}	89294.068	4.6(10) 5.2(10) ^c 4.8 ^b	S00 GV85 AM00	3.78 3.24 3.04	OH10 TW AM05

^aReferences: AL77 – Andersen and Lindgård [16]; AM00 – Alonso-Medina and Colón [34]; AM05 – Alonso-Medina et al. [36] (Cowan code); D80 – David et al. [27]; GV85 – Gorshkov and Verolainen [37]; OH10 – Oliver and Hibbert [14]; S00 – Schectman et al. [15]; TW – this work (Cowan code).

^bDetermined from the sum of measured radiative rates.

^cOriginal estimate of uncertainty doubled (see text).

Gorshkov and Verolainen [37] determined the lifetimes of the two 5s²4f ²F^o_{5/2,7/2} levels by using intersecting atomic and electron beams and a multichannel method of retarded coincidences. Although they reported very small uncertainties of ± 0.5 ns, their description of the experiment lacks any mention of an account for cascading effects. Therefore, in table 5 we have doubled their uncertainty estimate.

As can be seen from table 5, lifetimes calculated by Oliver and Hibbert [14] agree with all the best measurements within the uncertainties.

Our own calculations made with the Cowan codes (using the LSF parameters) are compared with the calculations of Oliver and Hibbert [14] in figure 5.

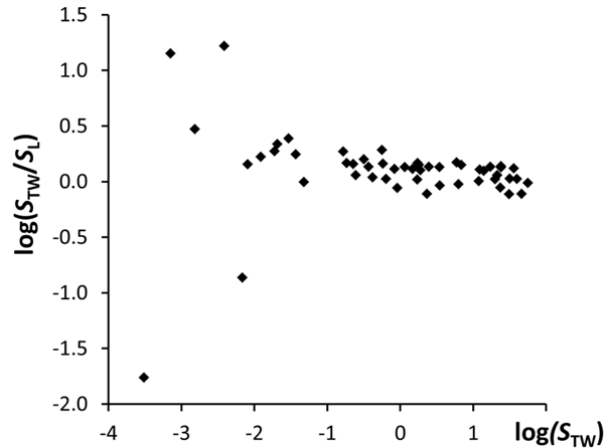


Figure 5. Comparison of line strengths calculated in the present work with Cowan's codes (S_{TW}) with those from fine-tuned calculations of Oliver and Hibbert in the length gauge (S_{L}).

For strong transitions with line strength $S > 0.5$, our calculations agree with those of Oliver and Hibbert [14] to 28 % on average. For weaker transitions, the results of Cowan's codes deviate from Oliver and Hibbert [14] by more than a factor of two on average. Calculations of Alonso-Medina et al. [36], also using a parametric fitting with Cowan's codes, are of similar quality, although they display somewhat larger deviations from Oliver and Hibbert [14] (about 30 % on average for $S > 1$, and 70 % for weaker transitions). We note that the f - and A -values given by Alonso-Medina et al. [36] in their table V for the $5s^2nf-5s^2n'g$ transitions are not consistent with each other and strongly disagree with our calculations.

Results of Oliver and Hibbert [14] also compare well with the relativistic all-order calculations of Safronova et al. [38]. These authors presented their results only for a few $5s^2ns-5s^2n'p$ and $5s^2np-5s^2n's$ transitions. They agree with Oliver and Hibbert [14] with an average deviation of 12 %, except for one $5s^25p^2P^{\circ}_{3/2}-5s^27s^2S_{1/2}$ transition (1219.083 Å), for which their S value is lower by a factor of 2.5.

Aside from a few discrepancies mentioned above, theoretical calculations of line strengths agree with each other, at least for strong transitions, and they agree reasonably well with the few available lifetime measurements. However, comparison with experimentally measured radiative rates (A -values) presents problems. The A -values were measured for several tens of transitions by Alonso-Medina and Colón [34], Schectman et al. [15], Miller et al. [39], Wujec and Weniger [40], and Wujec and Musielok [41]. Experimental line strengths reported in these papers are compared with the critically evaluated theoretical data in figure 6. Only a few measured values agree with theory within the claimed measurement uncertainties. The greatest discrepancies are observed for the weakest lines measured by Alonso-Medina and Colón [34]. It is difficult to identify the causes of the discrepancies. However, from the above analysis of the theoretical data, we conclude that the discrepancies originate in some flaws in the measurements. For this reason, we retained in table 1 only four experimental A -values, three from Alonso-Medina and Colón [34] and one from Miller et al. [39], and assigned greatly increased uncertainties to them.

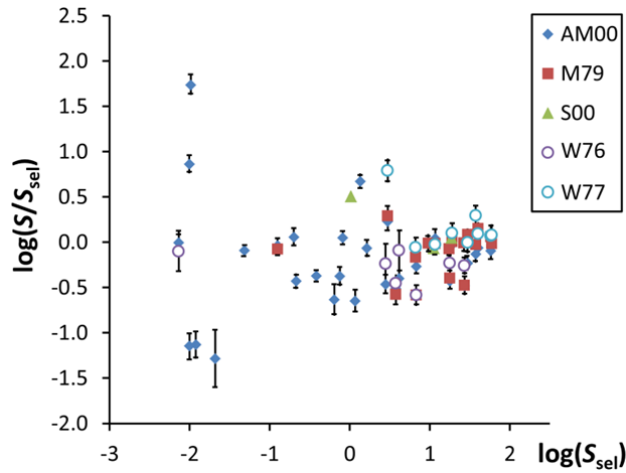


Figure 6. (Color online) Comparison of experimental line strengths S with selected theoretical data. The selected line strength S_{sel} were taken from Oliver and Hibbert [14] and from our calculations and have estimated uncertainties between 6 % and 35 %. The error bars correspond to claimed measurement uncertainties (one standard deviation). Key to experimental work: AM00 – Alonso-Medina and Colón [34]; M79 – Miller et al. [39]; S00 – Schectman et al. [15]; W76 – Wujec and Musielok [41]; W77 – Wujec and Weniger [40].

We included in table 1 four lines at 2442.7 Å, 2486.6 Å, 2592.3 Å, and 3351.3 Å, for which Alonso-Medina and Colón [34] reported measured A -values. Since these authors did not attempt to accurately measure the wavelengths, and these lines were not reported by other authors, the wavelengths given in the column λ_{obs} are actually the rounded Ritz wavelengths. We note that the last two of these lines, as well as two other lines reported by Alonso-Medina and Colón [34] at 2592.6 Å and 3351.9 Å, were incorrectly identified by these authors.

We also included in table 1 one unobserved parity-forbidden line corresponding to the transition between the levels of the ground term. Our predicted wavelength for this far-infrared line is 23521.08(23) Å.

According to calculations of Biémont et al. [35], Warner [42], and Garstang [43], this line is dominated by the magnetic dipole (M1) transition. The A -values calculated for this M1 transition in these works agree with each other within 1 %. The A -value for the electric quadrupole transition, 2.893 s^{-1} [35], amounts to only 0.4 % of the M1 decay rate and can be neglected in most applications.

Since the statistical distribution of both measured and calculated A -values is far from normal, uncertainties of the adopted A -values are specified in table 1 with a letter code instead of numerical values. The letter code is explained in table 6.

Table 6. Transition probability uncertainty code

Letter	Uncertainty in A -value	Uncertainty in $\log(gf)$
AAA	$\leq 0.3 \%$	≤ 0.0013
AA	$\leq 1 \%$	≤ 0.004
A+	$\leq 2 \%$	≤ 0.009
A	$\leq 3 \%$	≤ 0.013
B+	$\leq 7 \%$	≤ 0.03
C+	$\leq 18 \%$	≤ 0.08
C	$\leq 25 \%$	≤ 0.11
D+	$\leq 40 \%$	≤ 0.18
D	$\leq 50 \%$	≤ 0.24
E	$> 50 \%$	> 0.24

7. Conclusion

A comprehensive interpretation of the spectrum of singly ionized tin (Sn II) is presented here. The analysis covers the wavelength region 887 Å to 10611 Å. The earlier reported levels of even parity configurations, $5s^2nd$ ($n = 5-11$), $5s^2ns$ ($n = 6-11$), $5s^2ng$ ($n = 6-11$) and $5s5p^2$ have been confirmed with minor improvements in their level values, while the $5s^25g$ level has been newly identified. The ambiguity in the level values of $^2S_{1/2}$ and $^2P_{1/2}$ of the $5s5p^2$ configuration has been resolved. In odd parity, the reported levels of the $5s^2np$ ($n = 5-9$) and $5s^2nf$ ($n = 4-6$) configurations have been verified. Sixty-nine levels are now known in Sn II. Among these, eight are new, and for 11 levels previous values and/or interpretations have been revised. The level values, which are based on the identification of about 200 spectral lines, have been optimized in a least-squares fitting procedure. About 70 of these lines were measured by us either for the first time or with a significantly improved precision. With these improved data, the ionization energy of Sn II has been determined more accurately. For 140 transitions out of total 215, we give a critically evaluated value of transition probability with an estimated uncertainty. About 40 % of these transition probabilities have an accuracy C+ ($\leq 18 \%$) or better.

Acknowledgements

KH would like to duly acknowledge the Council of Scientific and Industrial Research (CSIR) for giving financial support through the Senior Research Fellowship (SRF) Scheme. AT is thankful to the kind hospitality of late Prof. Y N Joshi and St. Francis Xavier University, Antigonish (Canada) during the recording of tin spectra.

References

- [1] Hobbs L M, Welty D E, Morton D C, Spitzer L and York D G 1993 *Astrophys. J.* **411** 750
- [2] Sofia U J, Meyer D M and Cardelli J A 1999 *Astrophys. J.* **522** L137
- [3] Foster A R, Counsell G F and Summers H P 2007 *J. Nucl. Mater.* 363 152
- [4] Moore C E 1958 *Atomic Energy Levels, National Bureau of Standards Circular 467* vol. III (Washington, DC: US Govt. Printing Office)
- [5] Kramida A, Ralchenko Yu., Reader J and NIST ASD Team 2012 *NIST Atomic Spectra Database, v.5.0*, National Institute of Standards and Technology, Gaithersburg, MD, USA. Available from: <http://physics.nist.gov/ASD>.

- [6] McCormick W W and Sawyer R A 1938 *Phys. Rev.* **54** 71
- [7] Green J B and Loring R A 1927 *Phys. Rev.* **30** 574
- [8] Narayan A L and Rao K R 1927 *Nature Comm.* **120** 120
- [9] Lang R J 1930 *Phys. Rev.* **35** 445
- [10] Brill W G 1964 *The Arc Spectrum of Tin*, Ph. D. thesis, Purdue University, Lafayette, IN, USA, 119 pp.
- [11] Wu C M 1967 *The Atomic Spark Spectra of Tin, Sn III, Sn IV, Sn V*, Master thesis, University of British Columbia, Canada
- [12] Lysaght M A, Kilbane D, Cummings A, Murphy N, Dunne P, O'Sullivan G, Kampen P van, Costello J T and Kennedy E T 2005 *J. Phys. B* **38** 4247
- [13] Duffy G, van Kampen P and Dunne P 2001 *J. Phys. B: At. Mol. Opt. Phys.* **34** 3171
- [14] Oliver P and Hibbert A 2010 *J. Phys. B: At. Mol. Opt. Phys.* **43** 074013
- [15] Schectman R M, Cheng S, Curtis L J, Federman S R, Fritts M C and Irving R E 2000 *Astrophys. J.* **542** 400
- [16] Andersen T and Lindgård A 1977 *J. Phys. B: At. Mol. Opt. Phys.* **10** 2359
- [17] Alonso-Medina A, Colón C and Martínez H C 2003 *Astrophys. J.* **595** 550
- [18] Kelly R L 1987 *J. Phys. Chem. Ref. Data* **16** 651
- [19] Cowan R D 1981 *The Theory of Atomic Structure and Spectra* (Berkeley, CA: University of California Press) and Cowan code package for Windows by A. Kramida, available from <http://das101.isan.troitsl.ru/COWAN>
- [20] Sansonetti J E and Martin W C 2005 *J. Phys. Chem. Ref. Data* **34** 1559
- [21] Connerade J P and Baig M A 1981 *J. Phys. B: At. Mol. Opt. Phys.* **14** 29
- [22] Colón C and Alonso-Medina A 2004 *Astron. Astrophys.* **422** 1109
- [23] Tauheed A, Joshi Y N and Rana T 2000 *Physica Scripta* **61** 696
- [24] Tauheed A, Zafaran A F and Joshi Y N 1999 *J. Phys. B: At. Mol. Opt. Phys.* **32** 2917
- [25] Tauheed A, Joshi Y N and Pinnington E H 1998 *J. Phys. B: At. Mol. Opt. Phys.* **31** 393
- [26] Kramida A E 2011 *Comput. Phys. Commun.* **182** 419
- [27] David D, Hamel J and Barrat J-P 1980 *Opt. Commun.* **32** 241
- [28] Kramida A 2013 *Fusion Sci. Technol.* **63** 313
- [29] Kramida A 2013 *J. Res. Natl. Inst. Stand. Technol.* **118** 52
- [30] Kramida A 2013 *J. Res. Natl. Inst. Stand. Technol.* **118** 168
- [31] Sansonetti C J 2005 *Computer programs RITZPL and POLAR*, private communication
- [32] Forrest L F, James G K, Ross K J, Wilson M and Pantinakis A 1985 *J. Phys. B: At. Mol. Opt. Phys.* **18** 3123
- [33] Dembczynski J and Wilson M 1988 *Z. Phys. D* **8** 329
- [34] Alonso-Medina A and Colón C 2000 *Physica Scripta* **61** 646
- [35] Biémont E, Hansen J E, Quinet P and Zeippen C J 1995 *Astron. Astrophys., Suppl. Ser.* **111** 333
- [36] Alonso-Medina A, Colón C and Rivero C 2005 *Physica Scripta* **71** 154
- [37] Gorshkov V N and Verolainen Ya F 1985 *Opt. Spectrosc.* **59** 694
- [38] Safronova U I, Safronova M S and Kozlov M G 2007 *Phys. Rev. A* **76** 022501
- [39] Miller M H, Roig R A and Bengtson R D 1979 *Phys. Rev. A* **20** 499
- [40] Wujec T and Weniger S 1977 *J. Quant. Spectrosc. Radiat. Transfer* **18** 509
- [41] Wujec T and Musielok J 1976 *Astron. Astrophys.* **50** 405
- [42] Warner B 1968 *Z. Astrophys.* **69** 399
- [43] Garstang R H 1964 *J. Res. Nat. Bur. Stand., Sect. A* **68**(1) 61